Cluster Degrees of Freedom in Heavy-Nucleus Decay and Structure

Yibin Qian

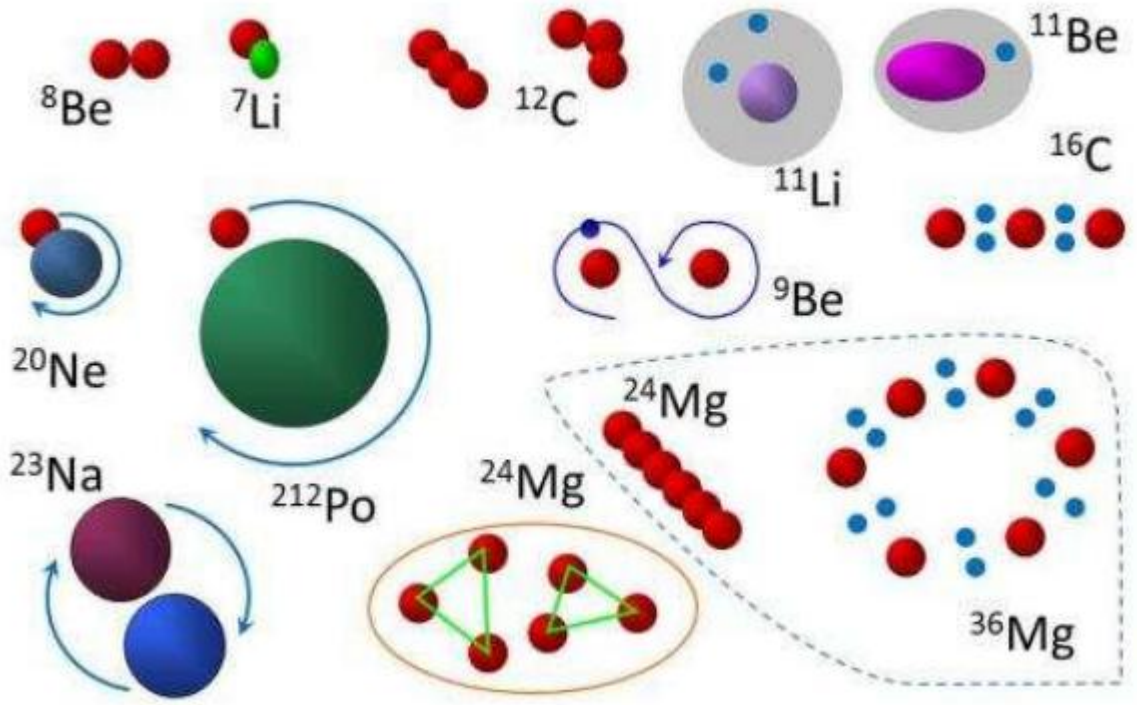
Nanjing University of Science and Technology

14th ITP/CAS-BLTP/JINR, 2026.10.18-23, Nanjing



Outline

- Research background
  1. Cluster phenomena in nucl
  2. α decay of nuclei
- α and 2α decay of nuclei
- Cluster structure in heavy nuc
- Summary



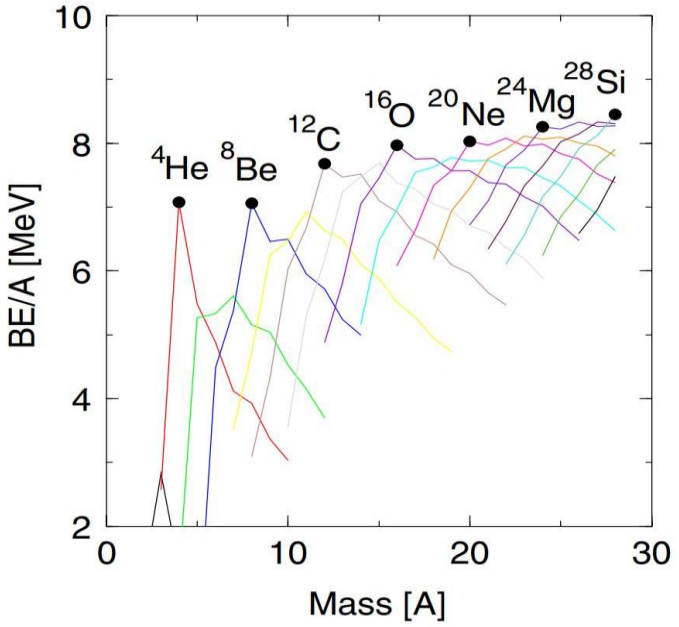
Adapted from C. Beck, J. Phys.: Conf. Ser. 569, 012002 (2014)

PART 01

1. Introduction
2. α and 2α decay of nuclei
3. Cluster structure in heavy nuclei
4. Outlook

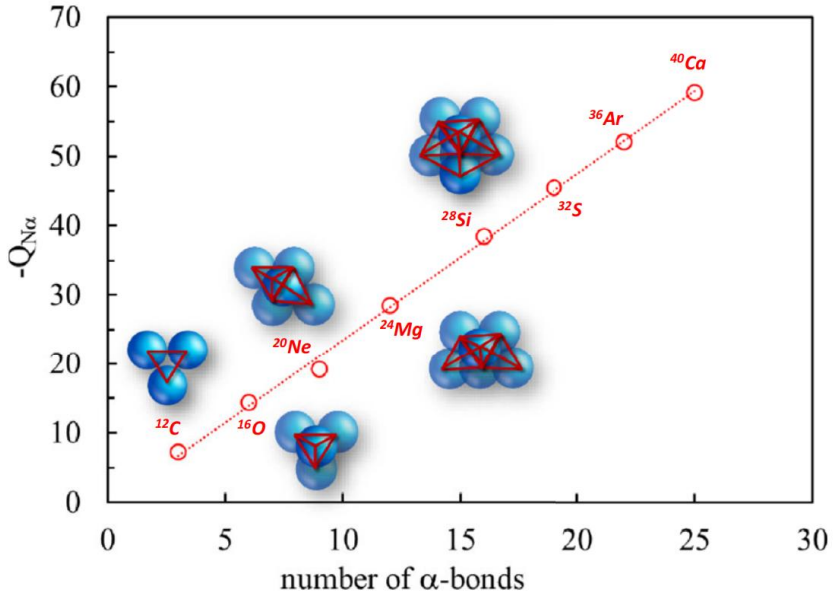
1. Background: early cluster picture of nuclei

南京理工大学 物理学院
SCHOOL OF PHYSICS , NANJING UNIVERSITY OF SCIENCE&TECHNOLOGY



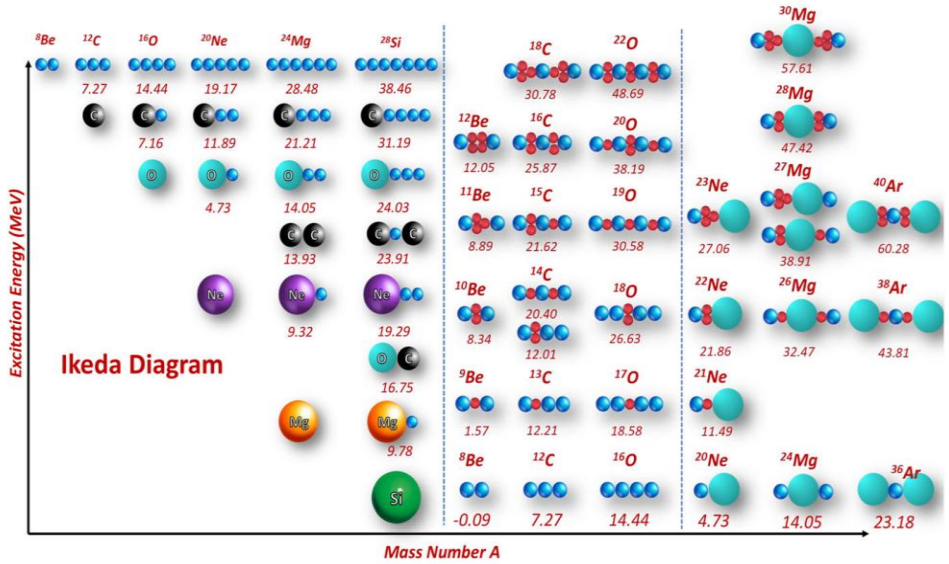
B.E./nucleon vs. mass number

M. Freer, Rep. Prog. Phys. **70**, 2149 (2007)



B.E. vs. number of α clusters

L. R. Hafstad, et al., Phys. Rev. **54**, 681 (1938)



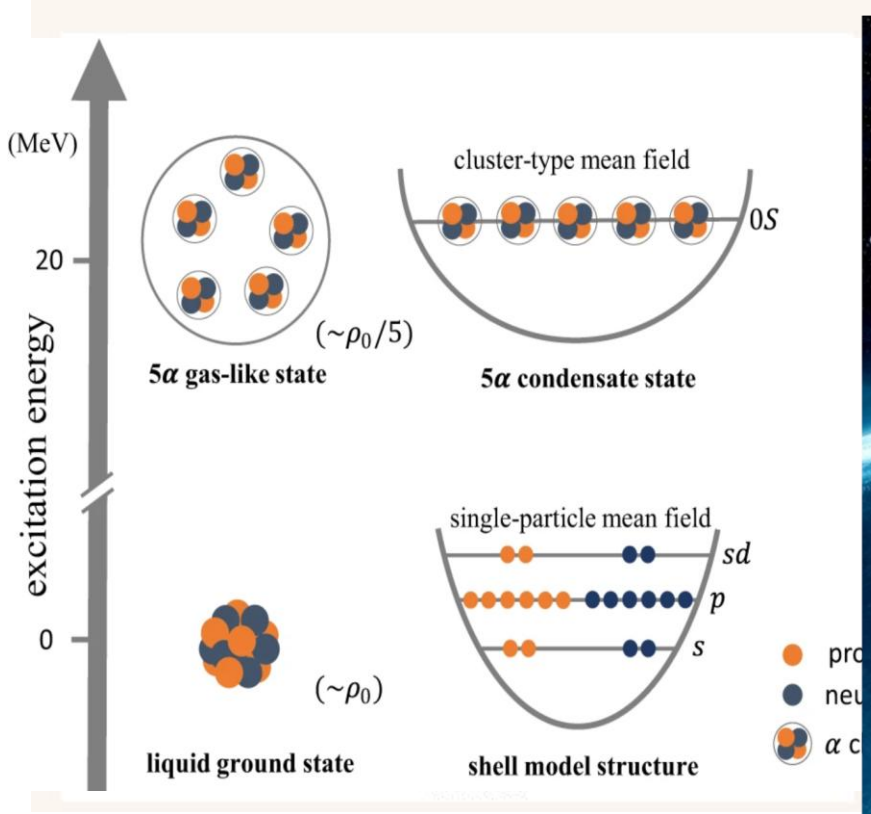
Ikeda diagram: cluster DOF in neutron-rich nuclei

K. Ikeda, et al., Theor. Phys. Suppl. E **68**, 464 (1968)
W. von Oertzen, et al., Phys. Rep. **432**, 43 (2006)

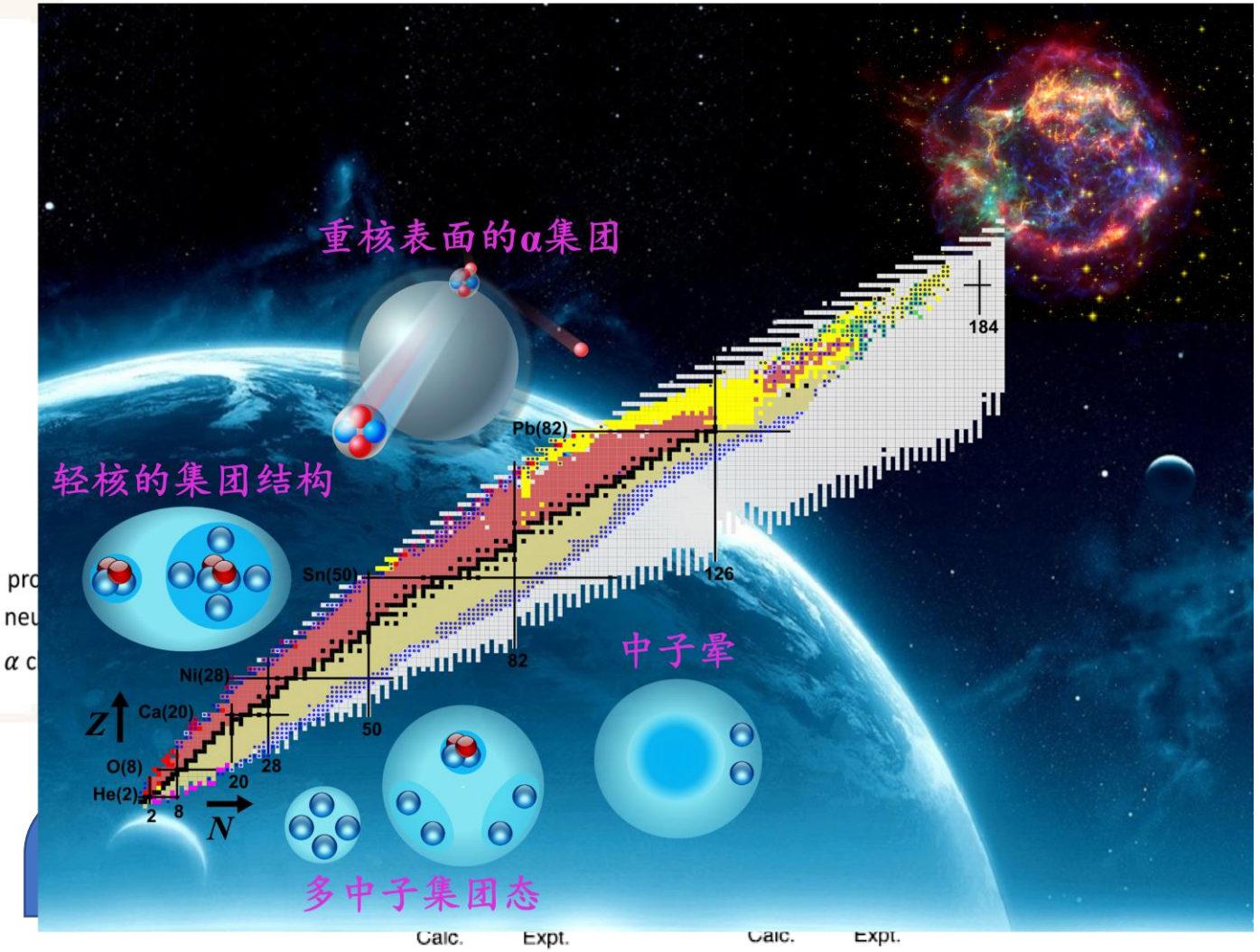
α clusters are regarded as basic building blocks of the atomic nucleus

1. Background: the cluster picture of nuclei

南京理工大学 物理学院
SCHOOL OF PHYSICS , NANJING UNIVERSITY OF SCIENCE&TECHNOLOGY



Cluster picture in light nuclei



B Zhou, Y Funaki, H Horiuchi, YG Ma, et al. Nat. Commun. 14, 8206 (2023).

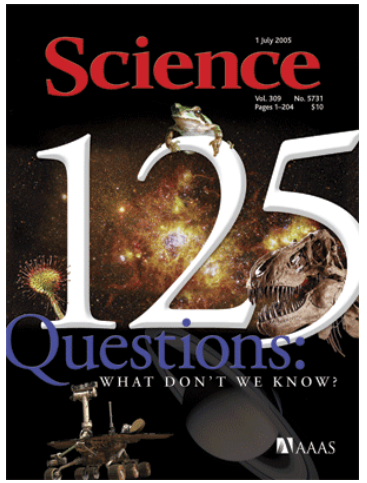
Cluster structure near doubly magic nuclei *M.A.Souza et al. PLB, 793 8 (2019)*

Adapted from Z. H. Yang

1. Background: α decay

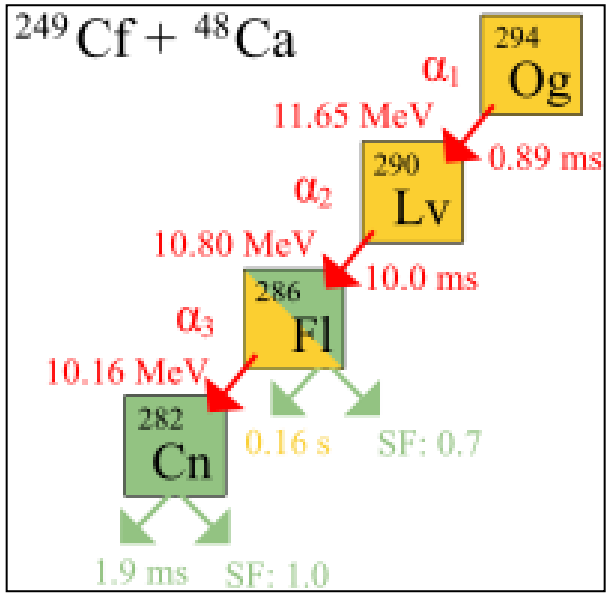
南京理工大学 物理学院
SCHOOL OF PHYSICS , NANJING UNIVERSITY OF SCIENCE&TECHNOLOGY

Marking its 125th anniversary, Science magazine posed 125 major scientific questions, spanning astronomy, physics, the life sciences, mathematics and beyond.

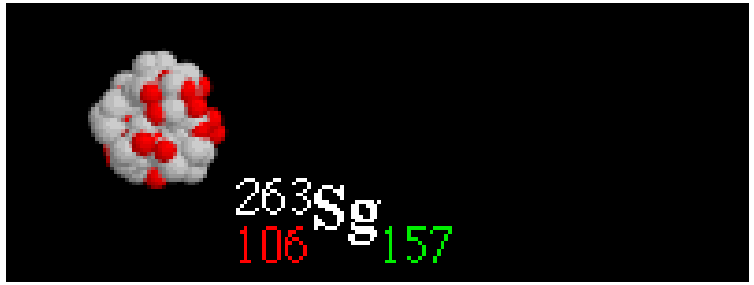


44. Are there stable elements with high atomic mass?

Are there stable high-atomic-number elements?



High-atomic-mass elements (new elements) are identified through α-cluster decay chains, and their stability is governed by the α-cluster decay lifetime.

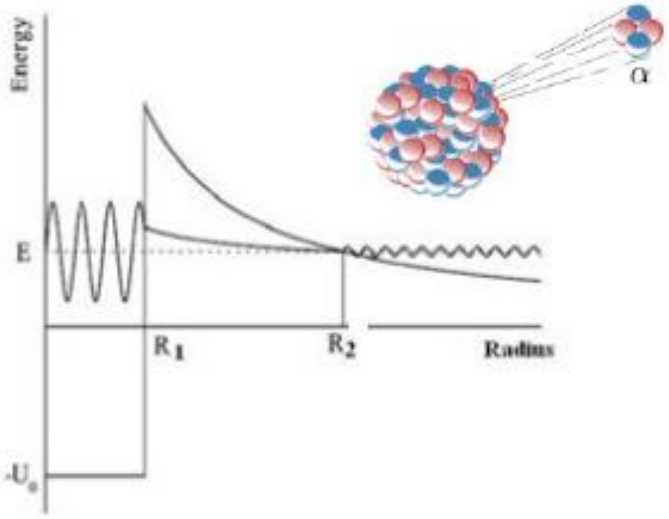


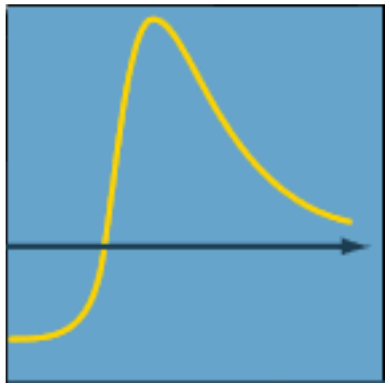
Theory of α decay

G. Gamow, Z. Phys. 51, 204 (1928).
R. W. Gurney and E. U. Condon, Nature 122, 439 (1928).

$$P = \exp\left\{-2\int_{R_1}^{R_2}\sqrt{\frac{2\mu}{\hbar^2}|V_C(r) - Q_\alpha|}\mathrm{d}r\right\}$$

$$\lambda = \ln 2/T = \nu S P_s$$





The α particle is not a basic constituent of the atomic nucleus

- α-particle model of the nucleus before the neutron **was discovered**
- Light nuclei can exhibit pronounced α clustering
- The Gamow theory carries no nuclear-structure information
- Spectroscopic factors / reduced widths **are not observables**

Theory of α decay

$$T_{1/2} = \frac{\hbar \ln 2}{\Gamma_c} = \frac{\ln 2}{\nu} \left| \frac{H_l^+(\chi, \rho)}{RF_c(R)} \right|^2$$

R. G. Thomas, Prog. Theor. Phys. 12, 253 (1954)

F(R) describes the α-particle formation amplitude inside the nucleus

Yes — it depends on the radius.



$$\mathcal{F}_l(R) = \int d\mathbf{R} d\xi_d d\xi_\alpha [\Psi(\xi_d)\phi(\xi_\alpha)Y_l(\mathbf{R})]^*_{J_m M_m} \Psi_m(\xi_d, \xi_\alpha, \mathbf{R}),$$

Shell model

H.J. Mang, PR 119, 1069 (1960); I. Tonozuka, A. Arima, NPA 323, 45 (1979).

BCS method

HJ Mang and JO Rasmussen, Mat. Fys. Medd. Dan. Vid. Selsk. (1962)

DS Delion, A. Insolia and RJ Liotta, PRC 46, 884 (1992).

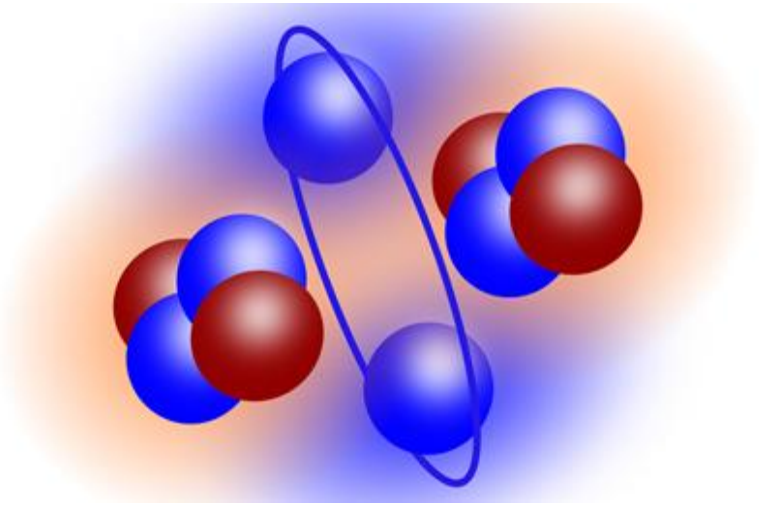
Theory of α decay

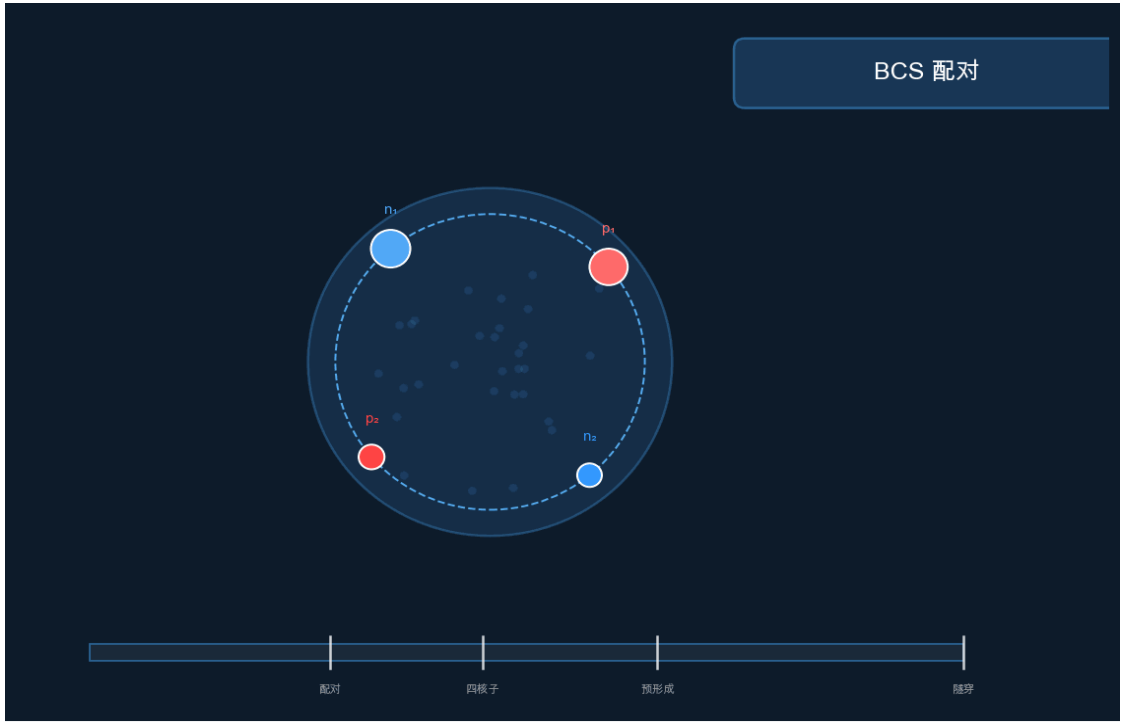
南京理工大学 物理学院
SCHOOL OF PHYSICS，NANJING UNIVERSITY OF SCIENCE&TECHNOLOGY

Effective α-decay models:

The formation amplitude F(R) is treated as Pα·μ(R); three general classes:

1. **Direct solution of the (coupled) radial Schrödinger equation for α + daughter**
2. **WKB approximation for the tunnelling probability**
3. **Phenomenological formulas**





PART 02

1. Introduction

2. α and 2α decay of nuclei

3. Cluster structure in heavy nuclei

4. Outlook

南京理工大学物理学院
SCHOOL OF PHYSICS , NANJING UNIVERSITY OF SCIENCE&TECHNOLOGY

Editors' Suggestion

New Isot

Z. Y. Zhang (
C. L.
M. D. Sun (孙
C. G. Wu (

[2]School
[4]Guangxi
[5]State Key L
[7]CAS Key Labora
[8]Center

Short-Lived α-

L. Ma (马龙),[1] Z. Y. Zl
M. H. Huang (黄明辉),[1]
H. B. Zhou (周厚兵),
W. X. Hua

Instit
[2]School of Nuclear
[3]School
[4]Guangxi Key Labor
[5]College of Material Scie
[6]I
[7]Sino-French Instit
[8]School
[9]C
[10]School of
[11]Center of Theoreti
[12]Synergetic Innovation

(Receive

Editors' Suggestion | Featured in Physics

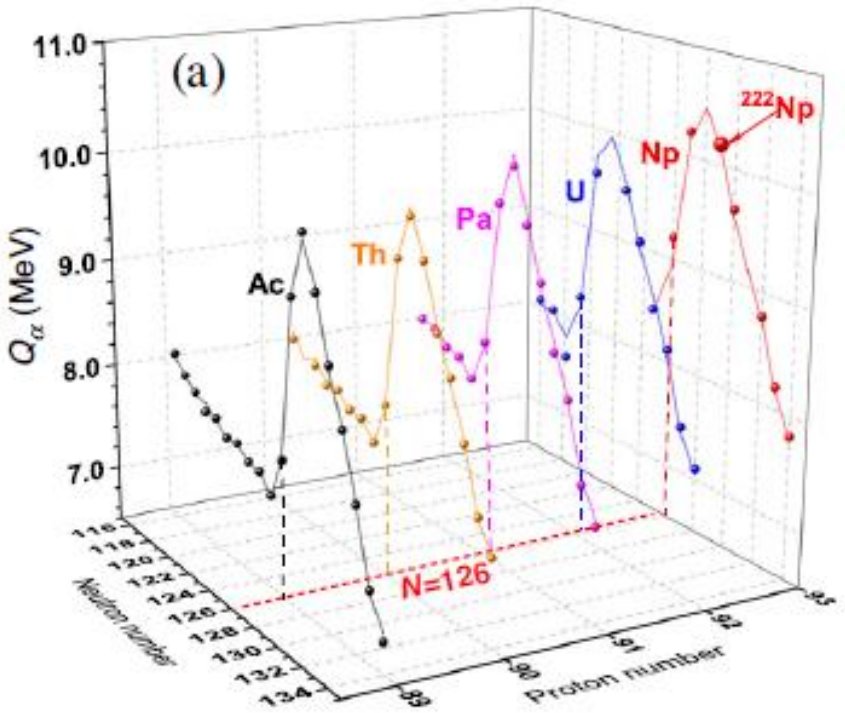
New α-Emitting Isotope ^{214}U and Abnormal Enhancement of α-Particle Clustering in Lightest Uranium Isotopes

Z. Y. Zhang (张志远),[1,2] H. B. Yang (杨华彬),[1] M. H. Huang (黄明辉),[1,2] Z. G. Gan (甘再国),[1,2,*] C. X. Yuan (袁岑溪),[3] C. Qi (亓冲),[4] A. N. Andreyev,[5,6] M. L. Liu (柳敏良),[1,2] L. Ma (马龙),[1] M. M. Zhang (张明明),[1] Y. L. Tian (田玉林),[1] Y. S. Wang (王永生),[1,2,7] J. G. Wang (王建国),[1] C. L. Yang (杨春莉),[1] G. S. Li (李广顺),[1] Y. H. Qiang (强赟华),[1] W. Q. Yang (杨维青),[1] R. F. Chen (陈若富),[1] H. B. Zhang (张宏斌),[1] Z. W. Lu (卢子伟),[1] X. X. Xu (徐新星),[1,2] L. M. Duan (段利敏),[1,2] H. R. Yang (杨贺润),[1,2] W. X. Huang (黄文学),[1,2] Z. Liu (刘忠),[1,2] X. H. Zhou (周小红),[1,2] Y. H. Zhang (张玉虎),[1,2] H. S. Xu (徐瑚珊),[1,2] N. Wang (王宁),[8] H. B. Zhou (周厚兵),[8] X. J. Wen (温小江),[8] S. Huang (黄山),[8] W. Hua (滑伟),[3] L. Zhu (祝龙),[3] X. Wang (王翔),[9] Y. C. Mao (毛英臣),[10] X. T. He (贺晓涛),[11] S. Y. Wang (王守宇),[12] W. Z. Xu (许文政),[12] H. W. Li (李弘伟),[12] Z. Z. Ren (任中洲),[13] and S. G. Zhou (周善贵)[14,15]

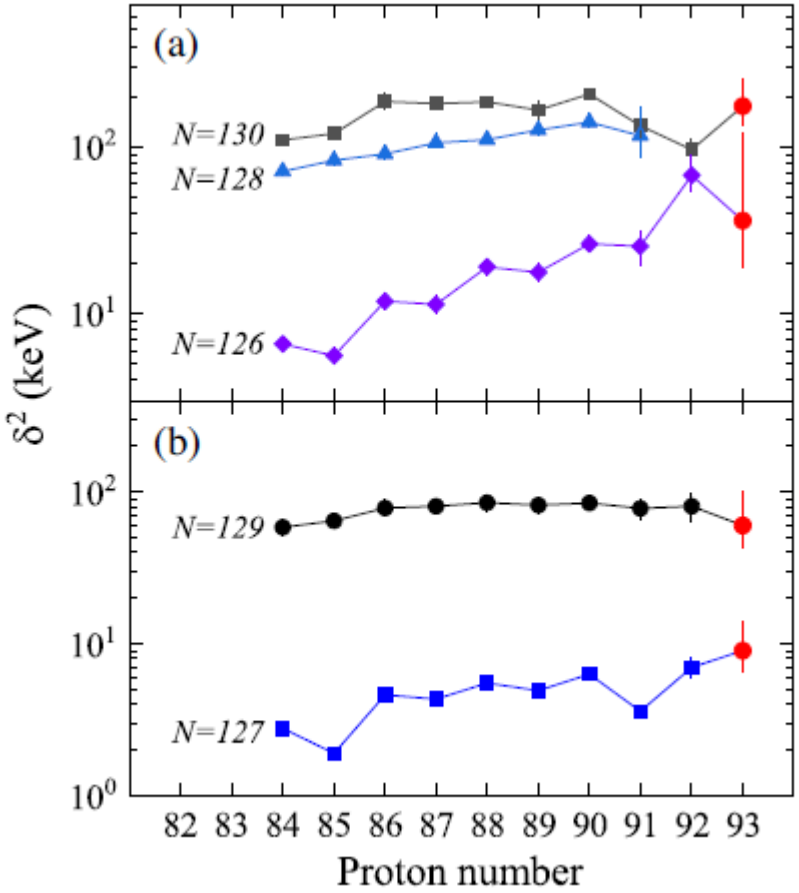
[1]*CAS Key Laboratory of High Precision Nuclear Spectroscopy, Institute of Modern Physics, Chinese Academy of Sciences, Lanzhou 730000, China*
[2]*School of Nuclear Science and Technology, University of Chinese Academy of Sciences, Beijing 100049, China*
[3]*Sino-French Institute of Nuclear Engineering and Technology, Sun Yat-Sen University, Zhuhai 519082, China*
[4]*Department of Physics, Royal Institute of Technology (KTH), Stockholm SE-10691, Sweden*
[5]*Department of Physics, University of York, York YO10 5DD, United Kingdom*
[6]*Advanced Science Research Center, Japan Atomic Energy Agency, Tokai, Ibaraki 319-1195, Japan*
[7]*School of Nuclear Science and Technology, Lanzhou University, Lanzhou 730000, China*
[8]*Guangxi Key Laboratory of Nuclear Physics and Technology, Guangxi Normal University, Guilin 541004, China*
[9]*State Key Laboratory of Nuclear Physics and Technology, School of Physics, Peking University, Beijing 100871, China*
[10]*Department of Physics, Liaoning Normal University, Dalian 116029, China*
[11]*College of Material Science and Technology, Nanjing University of Aeronautics and Astronautics, Nanjing 210016, China*
[12]*Shandong Provincial Key Laboratory of Optical Astronomy and Solar-Terrestrial Environment, School of Space Science and Physics, Institute of Space Sciences, Shandong University, Weihai 264209, China*
[13]*School of Physics Science and Engineering, Tongji University, Shanghai 200092, China*
[14]*CAS Key Laboratory of Theoretical Physics, Institute of Theoretical Physics, Chinese Academy of Sciences, Beijing 100190, China*
[15]*Center of Theoretical Nuclear Physics, National Laboratory of Heavy-Ion Accelerator, Lanzhou 730000, China*

(Received 15 January 2021; revised 25 February 2021; accepted 5 March 2021; published 14 April 2021)

2. α decay of nuclei: nuclear structure



α-decay energies along neutron-deficient isotope chains with Z = 89–93



Systematics of reduced decay widths for Po–Np

L. Ma, Z. Y. Zhang, Z. G. Gan, et al. PRL 125, 032502 (2020)

α-cluster effects in the uranium isotope chain — pairing correlations

南京理工大学 物理学院
SCHOOL OF PHYSICS , NANJING UNIVERSITY OF SCIENCE&TECHNOLOGY

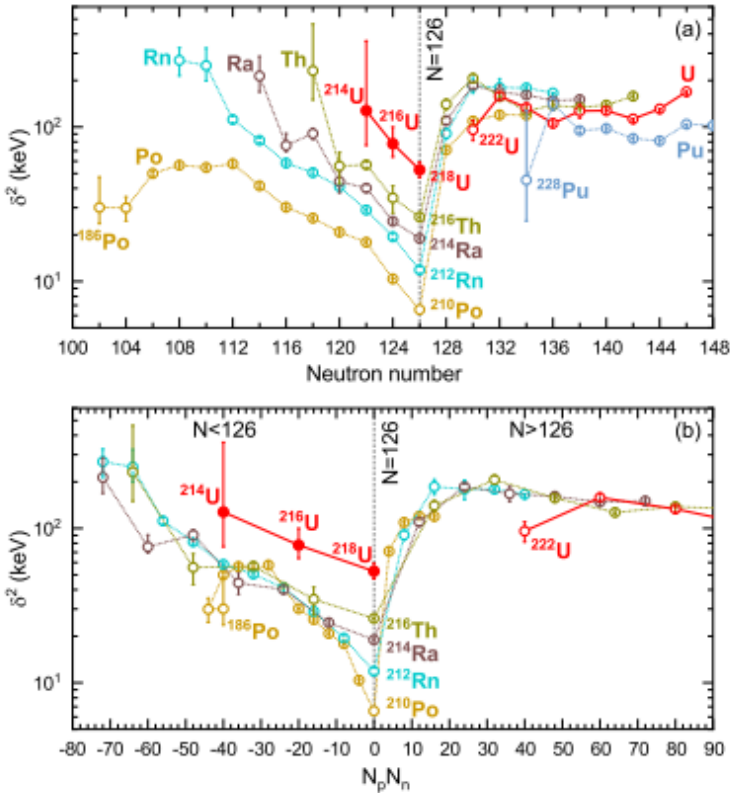


FIG. 3. (a) Systematics of reduced widths for g.s.-to-g.s. α decays of even-even $84 \leq Z \leq 94$ isotopes as a function of neutron number. The decay properties are taken from Refs. [11,12,42,50–53]. The values for ^{214,216,218}U from this work are shown by filled circles. The errors of reduced widths are only determined by half-life uncertainties. (b) Same as (a) but against N_pN_n for even-even Po to U isotopes. The N_p and N_n values are calculated relative to $Z = 82$ and $N = 126$ closed shells, respectively, with an exception of $^{186}_{84}Po_{102}$, for which $N_n = -20$, relative to the closest $N = 82$ neutron shell.

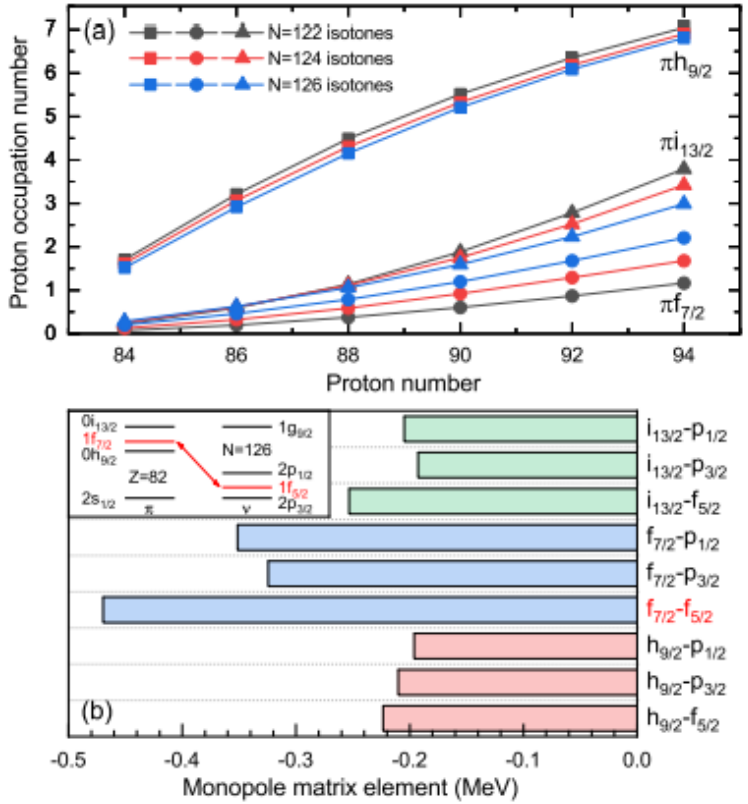
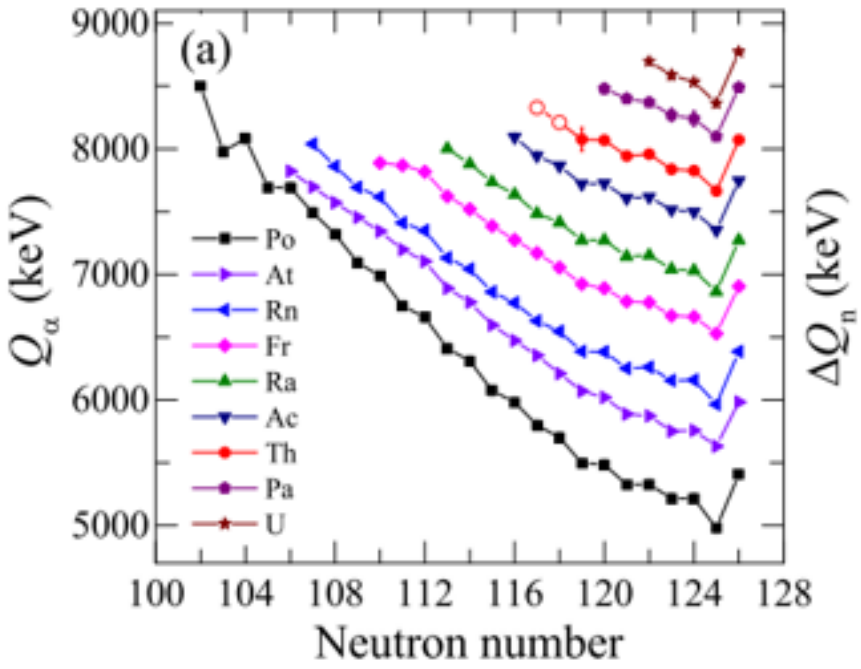


FIG. 4. (a) Calculated proton occupation numbers for the $\pi 0h_{9/2}$ (square), $\pi 1f_{7/2}$ (circle), and $\pi 0i_{13/2}$ (triangle) orbits in $N = 122$, 124, and 126 even-Z isotones of Po-Pu. (b) Monopole matrix elements of p-n interaction calculated for the $Z > 82$ and $N \leq 126$ nuclei. The inset in panel (b) shows the single-particle orbits near the ^{208}Pb doubly closed shells, and the strong interaction between the $1f_{7/2}$ protons and $1f_{5/2}$ neutrons is marked.

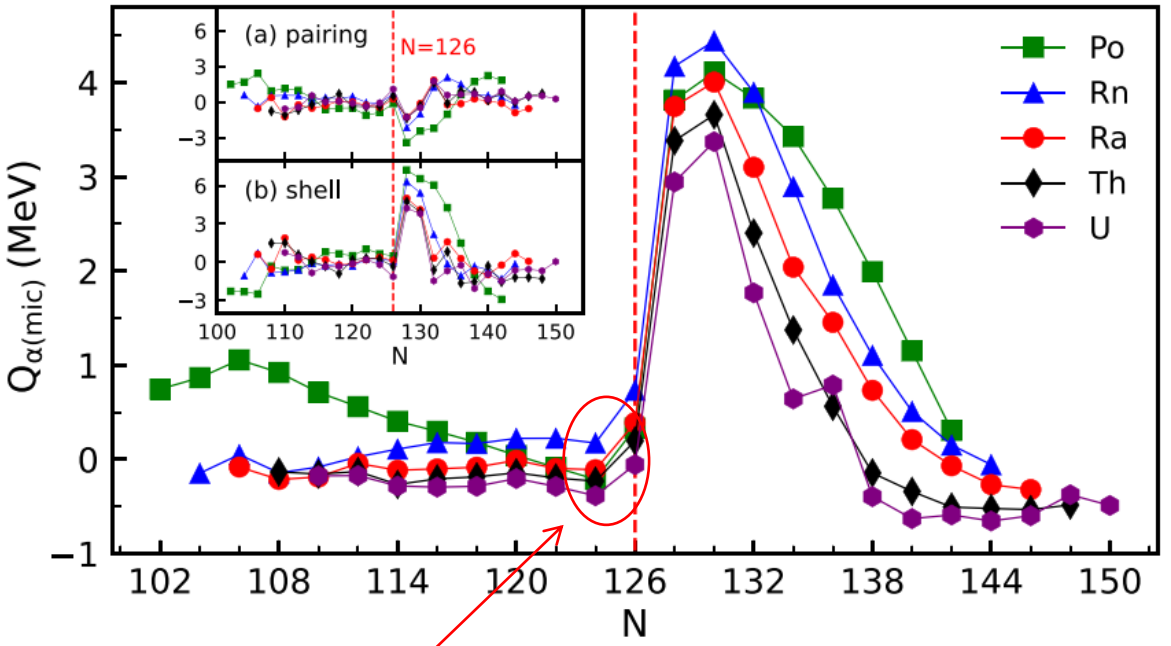
ZY Zhang, et al. PRL 126, 152502 (2021)

2. α decay of nuclei: decay energy



Odd-even staggering in the alpha decay energies of isotopes

H. B. Yang et al. Phys. Rev. C 105, L051302 (2022).

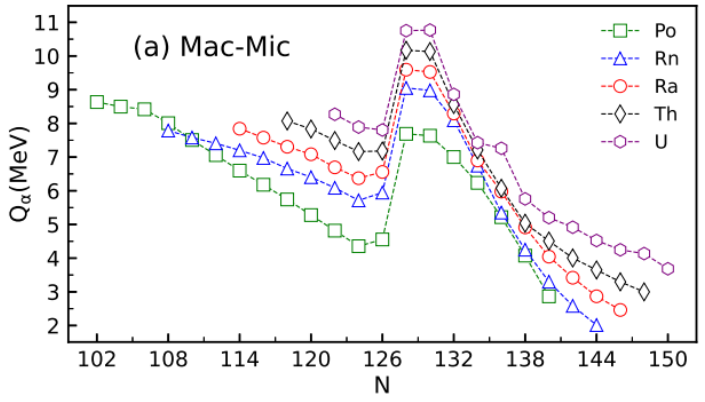


The increase of decay energy comes from the pairing correlation in the microscopic corrections

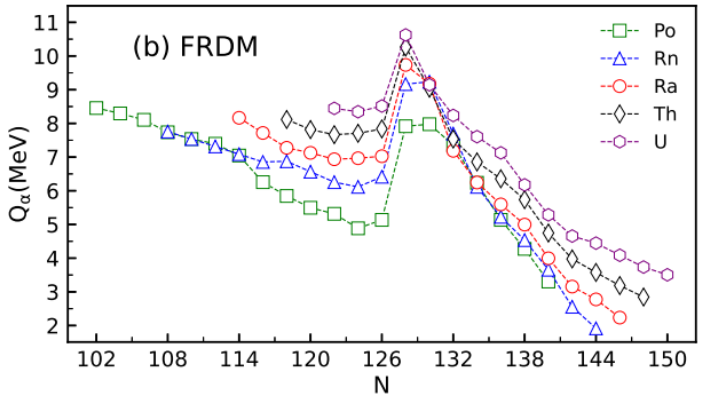
S. Tang, Y. Qian, and Z. Ren, Phys. Rev. C 112, 014308 (2025).

2. α decay of nuclei: decay energy

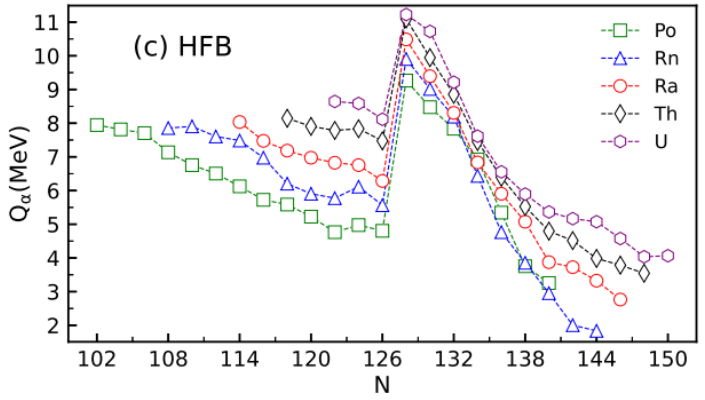
南京理工大学 物理学院
SCHOOL OF PHYSICS , NANJING UNIVERSITY OF SCIENCE&TECHNOLOGY



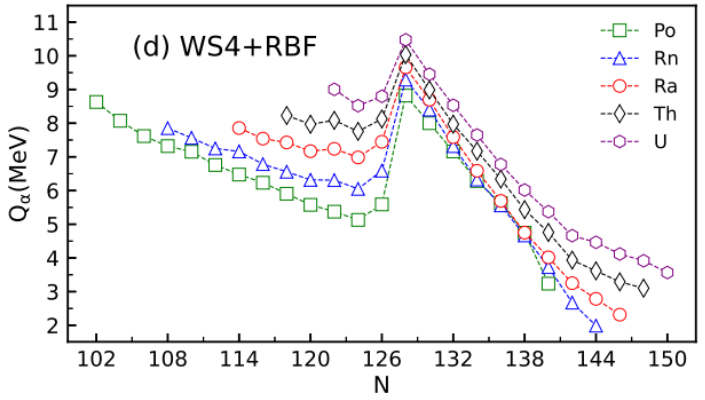
(a) Mac-Mic



(b) FRDM



(c) HFB



(d) WS4+RBF

Mac-Mic, FRDM and WS4+RBF reproduce the Q_α minimum at N = 124, whereas HFB places it at N = 126.

The position of the Q_α minimum is a sensitive probe of the shell–pairing balance in mass models.

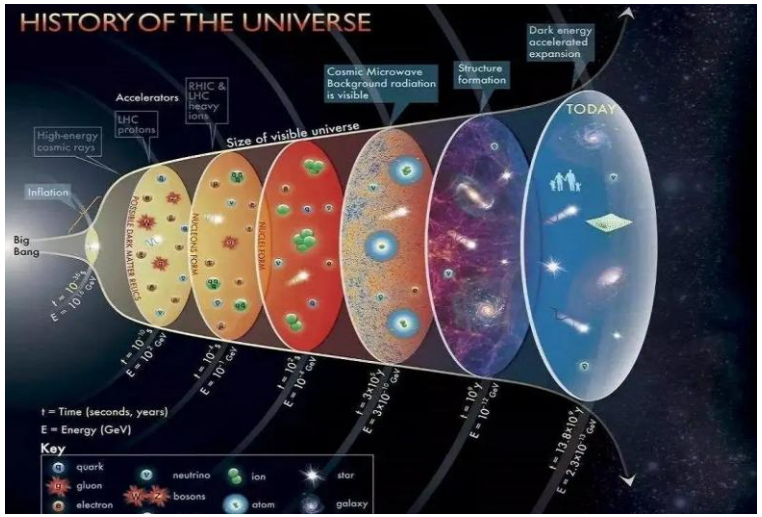
S. Tang, Y. Qian, and Z. Ren, Phys. Rev. C 112, 014308 (2025).

2. α decay of nuclei: the long-lived nuclide ^{146}Sm

南京理工大学 物理学院
SCHOOL OF PHYSICS , NANJING UNIVERSITY OF SCIENCE&TECHNOLOGY

Table 1 SLRs once existing in Solar System objects; shaded rows indicate SLRs with unconfirmed or uncertain abundances

Fractionation[a]	Parent nuclide	Half-life (Ma)[b]	Daughter nuclide	Estimated initial Solar System abundance	Objects found in	Reference(s)
Nebular	^{7}Be	53.22 ± 0.06 d	^{7}Li	$(6.1 \pm 1.3) \times 10^{-3} \times {}^{9}$Be	CAI	27
Nebular	^{10}Be	1.387 ± 0.0012	^{10}B	$(7.3 \pm 1.7) \times 10^{-4} \times {}^{9}$Be	CAIs	36; this article
Nebular, planetary	^{26}Al	0.717 ± 0.024	^{26}Mg	$(5.20 \pm 0.13) \times 10^{-5} \times {}^{27}$Al	CAIs, chondrules, achondrites	44, 45
Planetary	^{36}Cl	0.3013 ± 0.0015	^{36}S, ^{36}Ar	$(1.7–3.0) \times 10^{-5} \times {}^{35}$Cl	CAIs, chondrites	55
Nebular	^{41}Ca	0.0994 ± 0.0015	^{41}K	$4 \times 10^{-9} \times {}^{40}$Ca	CAIs	62
Nebular, planetary	^{53}Mn	3.7 ± 0.4	^{53}Cr	$(7 \pm 1) \times 10^{-6} \times {}^{55}$Mn	CAIs, chondrules, carbonates, achondrites	69
Nebular, planetary	^{60}Fe	2.62 ± 0.04	^{60}Ni	$(1.01 \pm 0.27) \times 10^{-8} \times {}^{56}$Fe	Achondrites, chondrites	79
Planetary	^{92}Nb	34.7 ± 2.4	^{92}Zr	$(1.66 \pm 0.10) \times 10^{-5} \times {}^{93}$Nb	Chondrites, mesosiderites	89
Planetary	^{97}Tc	4.21 ± 0.16	^{97}Mo	$<1 \times 10^{-6} \times {}^{92}$Mo	Iron meteorites	90
Planetary	^{98}Tc	4.2 ± 0.3	^{98}Ru	$<2 \times 10^{-5} \times {}^{96}$Ru	Iron meteorites	91
Planetary	^{107}Pd	6.5 ± 0.3	^{107}Ag	$(5.9 \pm 2.2) \times 10^{-5} \times {}^{108}$Pd	Iron meteorites, pallasites	94
Planetary	^{126}Sn	0.230 ± 0.014	^{126}Te	$<3 \times 10^{-6} \times {}^{124}$Sn	Chondrules, secondary minerals	101
Planetary	^{129}I	16.14 ± 0.12	^{129}Xe	$(1.35 \pm 0.02) \times 10^{-4} \times {}^{127}$I	Chondrules, secondary minerals	This article
Nebular	^{135}Cs	1.33 ± 0.19	^{135}Ba	$<2.8 \times 10^{-6} \times {}^{133}$Cs	CAIs, chondrites	109
Planetary	^{146}Sm	103 ± 5[c]	^{142}Nd	$(8.40 \pm 0.32) \times 10^{-3} \times {}^{144}$Sm	Planetary differentiates	114
Planetary	^{182}Hf	8.90 ± 0.09	^{182}W	$(1.018 \pm 0.043) \times 10^{-4} \times {}^{180}$Hf	CAIs, planetary differentiates	117
Planetary	^{205}Pb	17.0 ± 0.9	^{205}Tl	$(1.8 \pm 1.2) \times 10^{-3} \times {}^{204}$Pb	Chondrites	121
Planetary	^{244}Pu	81.3 ± 0.3	^{232}Th; fission	$(7.7 \pm 0.6) \times 10^{-3} \times {}^{238}$U	CAIs, chondrites	123
Nebular	^{247}Cm	15.6 ± 0.5	^{235}U	$(5.6 \pm 0.3) \times 10^{-3} \times {}^{235}$U	CAIs	4, 55



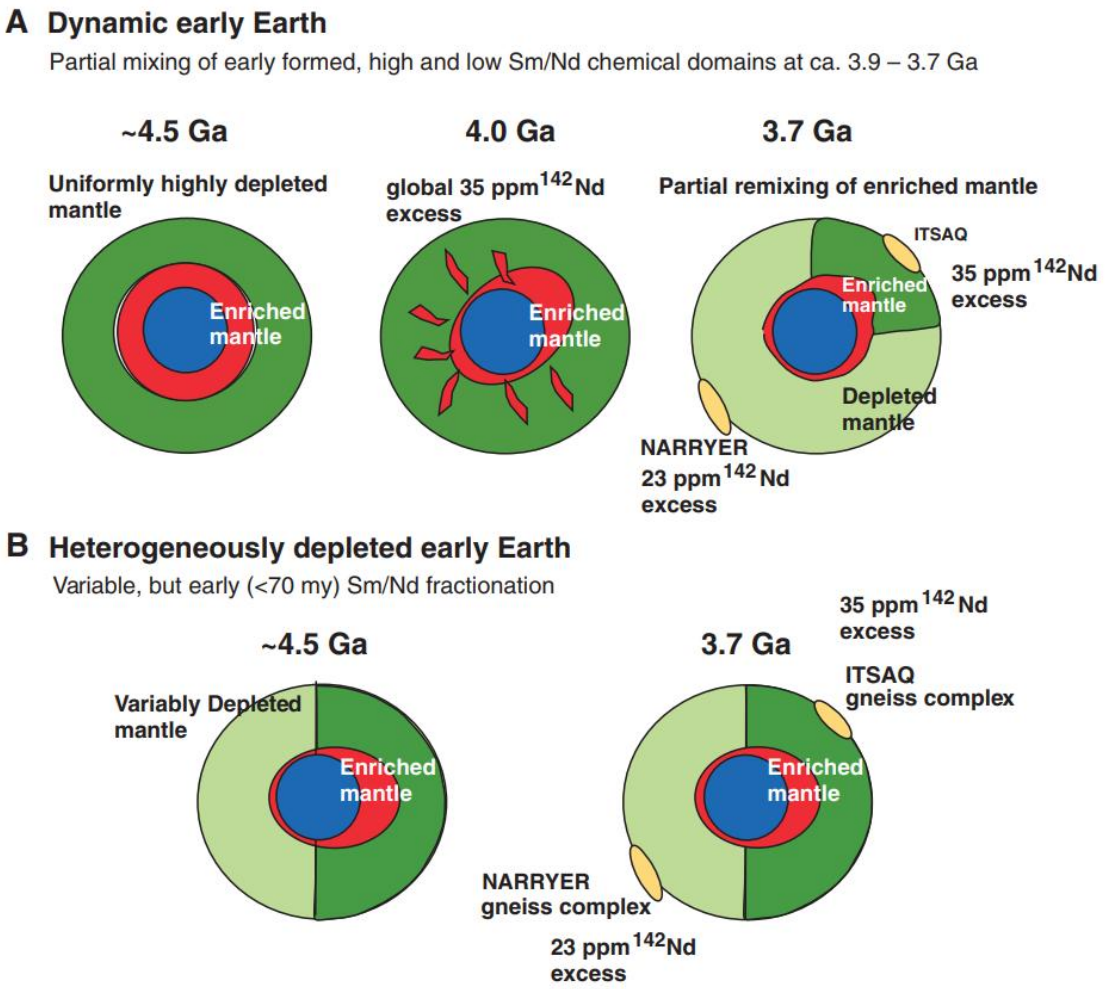
The ^{146}Sm–^{142}Nd chronometer often shows pronounced parent–daughter isotope fractionation during partial melting — fractionation large enough to produce isotopic differences among planetary reservoirs.

A. M. Davis, Annu. Rev. Earth Planet. Sci. 72, 339 (2022).

G. Caro, Annu. Rev. Earth Planet. Sci. 39, 31 (2011).

2. α decay of nuclei: the long-lived nuclide ^{146}Sm

南京理工大学物理学院
SCHOOL OF PHYSICS , NANJING UNIVERSITY OF SCIENCE&TECHNOLOGY



(A) Formation of uniform mantle (dark green) with high Sm/Nd early in Earth's history. A global mantle with uniformly high Sm/Nd within ~50 million years shows that the mantle was transient but survived locally until at least 3.6 Ga.

(B) Early-formed heterogeneous mantle. It will satisfy the ^{142}Nd constraints is that two (or more) mantle domains with variable Sm/Nd formed in the first ~50 My of Earth history and retained their distinct identities until at least 3.7 Ga.

V.C.Bennett,A.D.Brandon, and A.P.Nutman, Science 318,1907(2007)

2. α decay of nuclei: the long-lived nuclide ^{146}Sm

南京理工大学 物理学院
SCHOOL OF PHYSICS, NANJING UNIVERSITY OF SCIENCE&TECHNOLOGY

Measured $T_{1/2}$ spans 50–103 Ma

Recent values 92.0 ± 2.6 vs 103 ± 5 Ma are mutually inconsistent

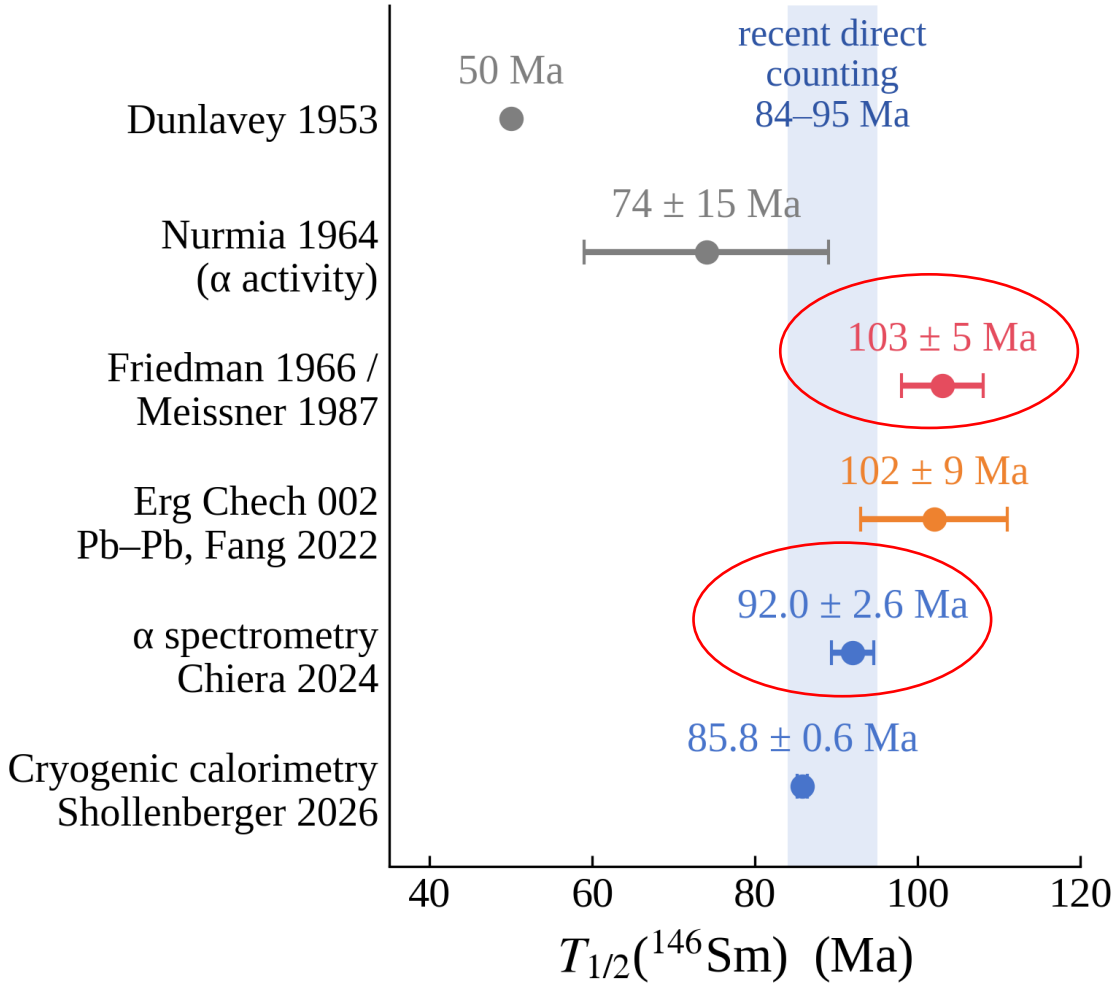
$T_{1/2}$ enters every ^{146}Sm–^{142}Nd age directly:

$$r_{ev} = r_0\, e^{-\lambda_{146} t_{ev}},\ \lambda_{146} = \ln 2 / T_{1/2}$$

$$t_{ev} = \frac{T_{1/2}}{\ln 2} \ln \frac{r_0(T_{1/2})}{r_{ev}}$$

Ages scale with $T_{1/2}$ at fixed r_0/r_{ev}

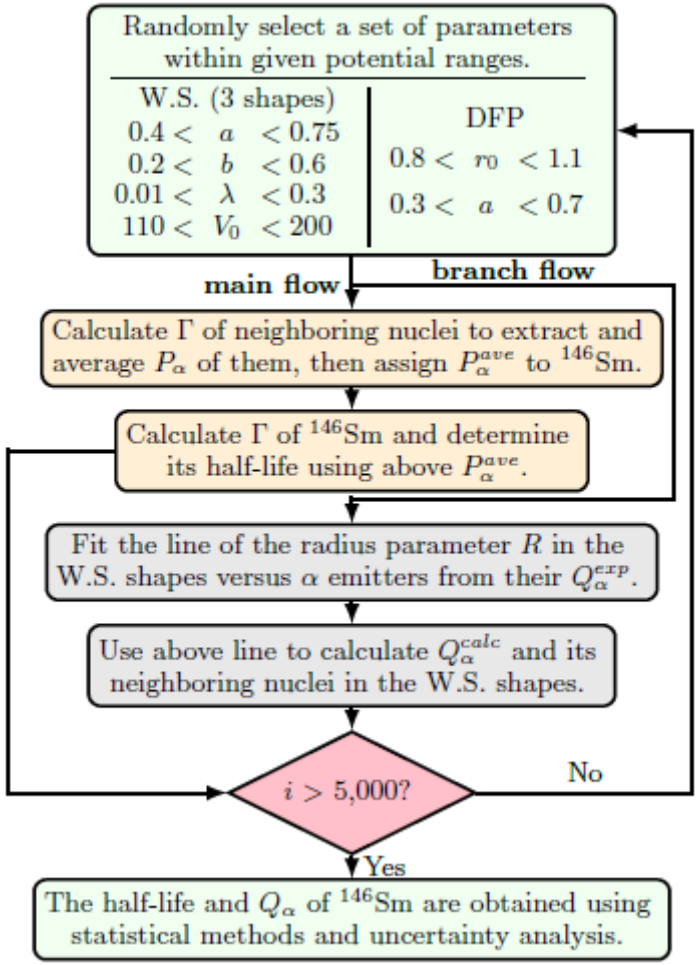
Motivation: a self-consistent microscopic $T_{1/2}$ with quantified uncertainty



S. Tang, Y. Qian, et al., in preparation (2026).

2. α decay of nuclei: the long-lived nuclide ^{146}Sm

南京理工大学 物理学院
SCHOOL OF PHYSICS , NANJING UNIVERSITY OF SCIENCE&TECHNOLOGY

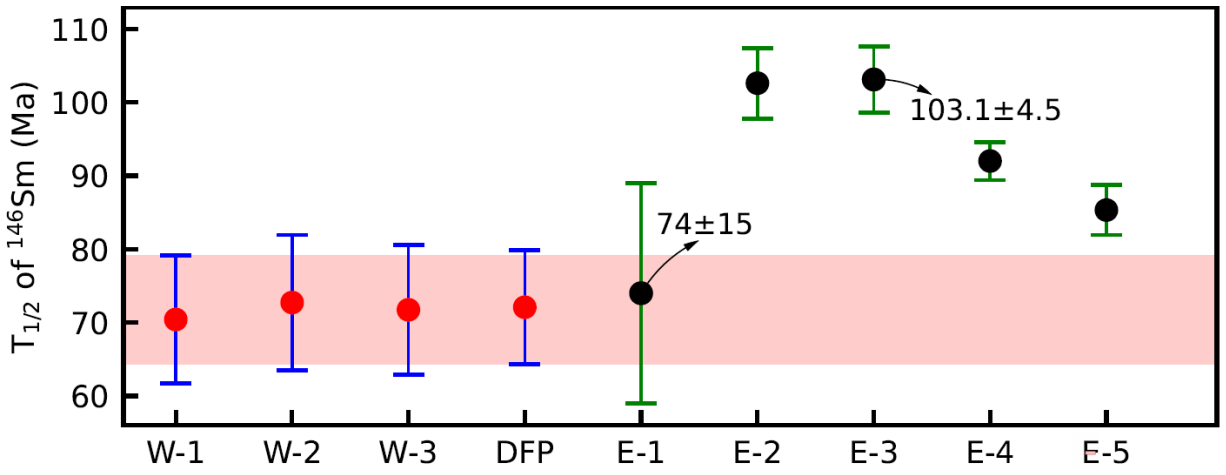


Flowchart of the calculation

1. Select the two most commonly used nuclear potentials

2. Randomly vary their parameters

3. Constrain them further with neighbouring α emitters

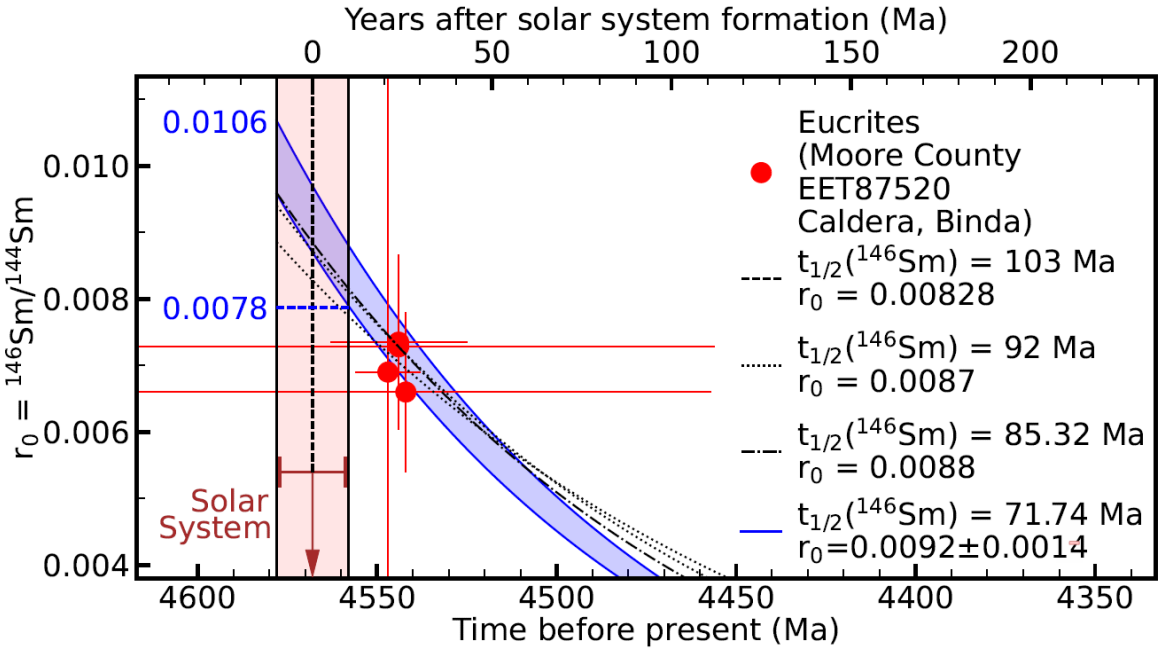


Calculated ^{146}Sm half-life

SL Tang, YB Qian, W Liu, ZZ Ren, PRC 111, L052801 (2025)

2. α decay of nuclei: the long-lived nuclide ^{146}Sm

南京理工大学物理学院
SCHOOL OF PHYSICS , NANJING UNIVERSITY OF SCIENCE&TECHNOLOGY



Distribution of the ^{146}Sm/^{144}Sm isotope ratio against two time axes: the upper x-axis is meteorite age (Myr after solar system formation, Ma), and the lower x-axis is solar system formation time (Myr before present).

$$\left(\frac{^{146}Sm}{^{144}Sm}\right)^i_T = \left(\frac{^{146}Sm}{^{144}Sm}\right)^i_{t_0} \exp(-\lambda_{146}(t_0 - T))$$

$$\left(\frac{^{142}Nd}{^{144}Nd}\right)^i_t = \left(\frac{^{142}Nd}{^{144}Nd}\right)^i_{t_0} + \left(\frac{^{146}Sm}{^{144}Sm}\right)^i_{t_0} \left(\frac{^{144}Sm}{^{147}Sm}\right)^{Std}_{t_p} \left(\frac{^{147}Sm}{^{144}Nd}\right)^i_{t_p} \left[1 - e^{-\lambda_{146}(t_0 - t)}\right]$$

Planetary body	Sample/Mantle differentiation event	Half-life (Ma)	Time after start of solar system formation (Ma)	
			$r_0 = 0.00828 \pm 0.00044$ is from Ref.[17]	$r_0 = 0.0094^{+0.0005}_{-0.0003}$ is reevaluated in this work
Moon[35]	Six lunar basalts / LMO solidification	103.1±4.5	218.1±24.1	$237.0^{+30.9}_{-27.8}$
		64.2±10.1	135.8±25.9	$147.8^{+32.5}_{-29.6}$
Moon[36]	Lunar array / LMO solidification	103.1±4.5	238.1±25.7	$257.0^{+32.6}_{-29.5}$
		64.2±10.1	148.2±28.0	$159.9^{+34.7}_{-31.8}$
Mars[37]	Enriched shergottites / Solidification of source	103.1±4.5	232.4±14.9	$251.3^{+21.3}_{-17.9}$
		64.2±10.1	144.7±24.3	$156.4^{+31.2}_{-28.2}$
Mars[38]	Enriched, depleted and intermediate shergottites / Solidification of source	103.1±4.5	63.2±8.9	$82.1^{+12.6}_{-9.3}$
		64.2±10.1	39.4±8.2	$51.1^{+14.0}_{-11.0}$
Earth[36]	Archean array, Isua, Greenland / Depleted source	103.1±4.5	166.1±10.7	$185.0^{+16.1}_{-12.7}$
		64.2±10.1	103.4±17.4	$115.1^{+24.2}_{-21.1}$
Earth[39]	Nuvvuagittuq greenstone belt, northern Quebec, Canada / Enriched sourcell	103.1±4.5	287.0±39.5	$305.9^{+46.8}_{-43.8}$
		64.2±10.1	178.6±37.1	$190.4^{+43.7}_{-40.9}$

Impact of different half-lives on early solar-system dating

SL Tang, YB Qian, W Liu, ZZ Ren, PRC 111, L052801 (2025)

2. 2α decay of nuclei: motivation

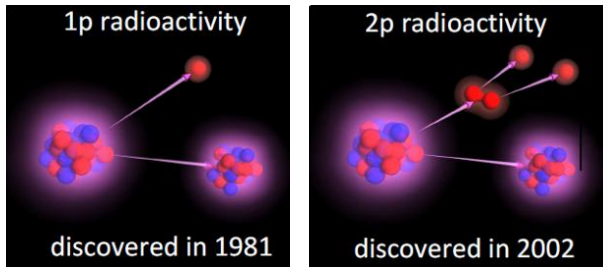
1896: Becquerel discovers radioactivity

1899–1908: Rutherford identifies α, β and γ rays

1911: Geiger–Nuttall law

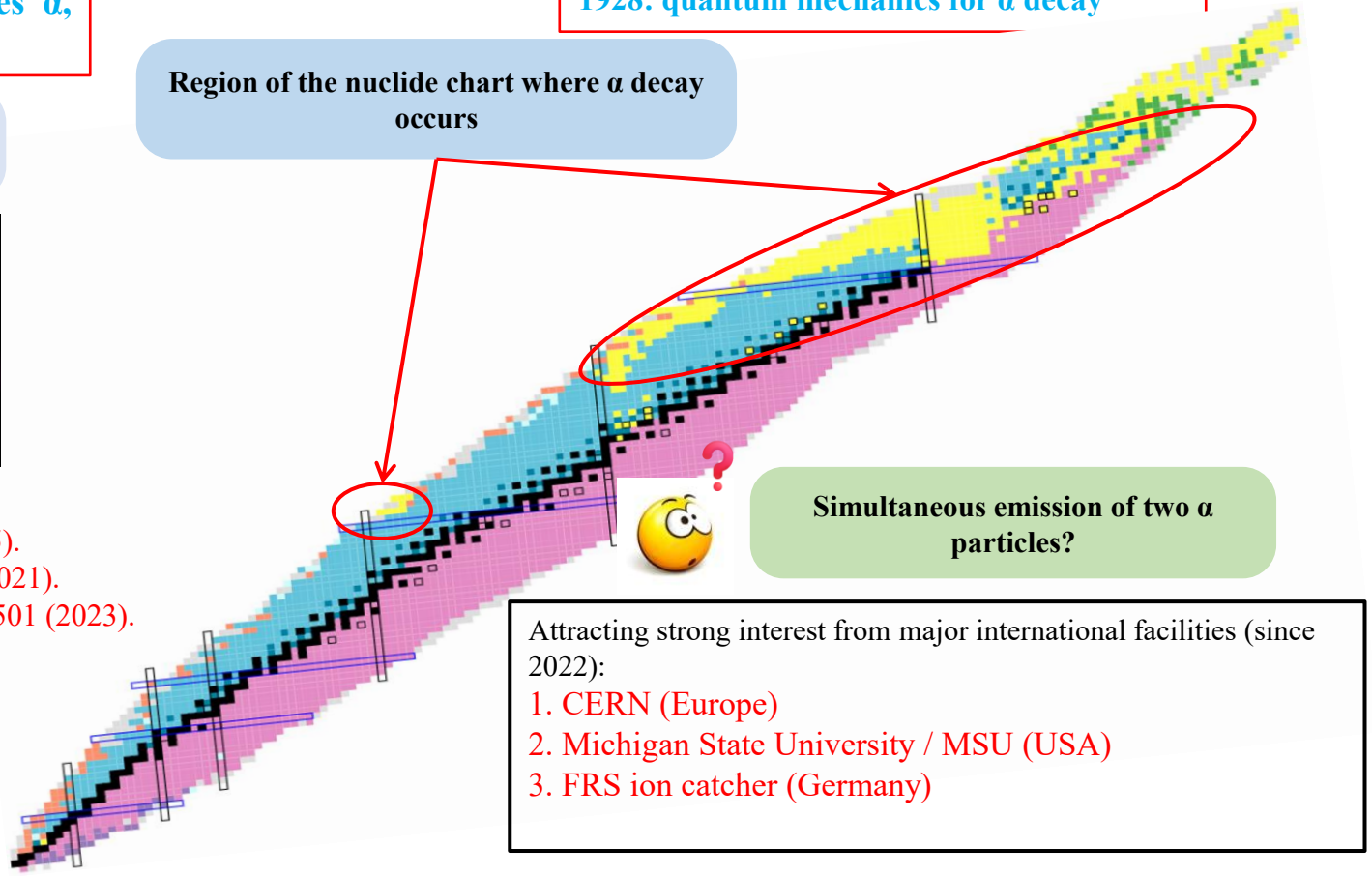
1928: quantum mechanics for α decay

Multi-particle radioactivity: opportunities for exotic nuclei



3p-5p decay:
L. Ni, *et. al.*, Phys. Lett. B 868, 139660 (2025).
Y. Jin, *et. al.*, Phys. Rev. Lett. 127, 262502 (2021).
S. M. Wang, *et. al.*, Phys. Rev. Lett. 131, 172501 (2023).

Region of the nuclide chart where α decay occurs



Simultaneous emission of two α particles?

Attracting strong interest from major international facilities (since 2022):
1. CERN (Europe)
2. Michigan State University / MSU (USA)
3. FRS ion catcher (Germany)

2. 2α decay of nuclei

南京理工大学 物理学院
SCHOOL OF PHYSICS , NANJING UNIVERSITY OF SCIENCE&TECHNOLOGY

Energy density functional (EDF)

$$S(L)=\int_{s_{in}}^{s_{out}}\frac{1}{\hbar}\sqrt{2\mathcal{M}_{\text{eff}}(s)[V_{\text{eff}}(s)-E_0]}ds$$

$$\mathcal{M}_{\text{eff}}(s)=\sum_{ij}\mathcal{M}_{ij}\frac{dq_i}{ds}\frac{dq_j}{ds}$$

Semi-phenomenological (UMADAC)

$$\Gamma_{\alpha\alpha}=\hbar\cdot\nu(Q_{\alpha\alpha})\cdot S_2\cdot t_{\alpha\alpha}(Q_{\alpha\alpha})$$

$$t_{\alpha\alpha}(Q_{\alpha\alpha})=\left[1+\exp\left(2\int_a^b dr\sqrt{f_{\alpha\alpha}(Q_{\alpha\alpha})}\right)\right]^{-1}$$

Liquid-drop-like model (MGLDM)

$$T_{1/2}=\left(\frac{\ln 2}{\lambda}\right)=\left(\frac{\ln 2}{\nu P_C P}\right)$$

$$\mathrm{P}=\exp\left\{-\frac{2}{\hbar}\int_{R_{in}}^{R_{out}}\sqrt{2B(r)[E(r)-E(\text{sphere})]}dr\right\}$$

L. Heitz, Ph.D. dissertation, Université Paris-Saclay, 2025.

Summary of Double Alpha decay Models

First Author	Config.	BR	Considered nuc		Year
D. Poenaru, et al., J. Physique Lett. 46, 591 (1985).	^{8}Be-like	$10^{-14.7}$–$10^{-12.6}$	Ac, Th isotopes	Pheno. Similar T values for 2α and ^{8}Be decay.	1985
V. I. Tretyak, Nucl. Phys. At. Energy 22, 121 (2021).	^{8}Be-like	—	^{231}Pa	Pheno. Very long half-lives (1.5×10^{33} yr for ^{231}Pa); not measurable.	2021
F. Mercier, et al., Phys. Rev. Lett. 127, 012501 (2021). J. Zhao, et al., Phys. Rev. C 107, 034311 (2023).	180°	$10^{-6.5}$–$10^{-7.5}$	$^{220-224}$Ra, $^{216-220}$Rn	EDF; benchmark on α and ^{14}C decays	2021 2022
K. P. Santhosh et al., Phys. Rev. C 104, 064604 (2021).	^{8}Be-like	$1.2\times10^{-14}-3.3\times10^{-17}$	Ra, Ru isotopes (in particular)	Pheno. Suspiciously short $T_{2\alpha}$ for ^{209}Bi; similar T for 2α and ^{8}Be.	2021
V. Denisov, Phys. Lett. B 835, 137569 (2022).	180°	$\approx 10^{-2.22}$	Rn,Ra isotopes (in particular)	Pheno. High BR for 2α, in particular for ^{230}Ra, unlikely	2022
D. Pathak, Eur. Phys. J. Plus 137, 1115 (2022)	^{8}Be-like	$\approx 10^{1-5}\times$ lower than Santhosh	^{220}Ra, ^{216},^{218}Rn (in particular)	Pheno. $10^{1\cdots1.5}$ lower than [419] for $^{220-224}$Ra and $^{216-220}$Rn.	2022

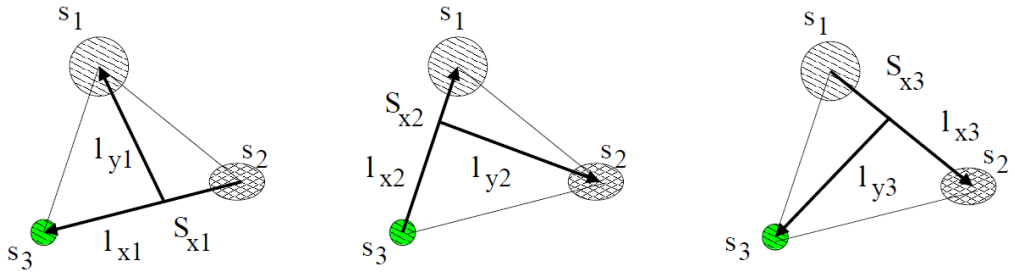
Existing theoretical predictions differ considerably

2α decay theory should respect three-body dynamics

2. 2α decay of nuclei

Obtaining ρ through the hyperspherical transformation:

$$\frac{\mathbf{r}_{ik}^2}{\rho^2} \equiv s_{ik}^2, \qquad mM \equiv \sum_{i<k} m_i m_k s_{ik}^2.$$



Jacobi coordinates (Faddeev)

Interaction potential including the α–α angle:

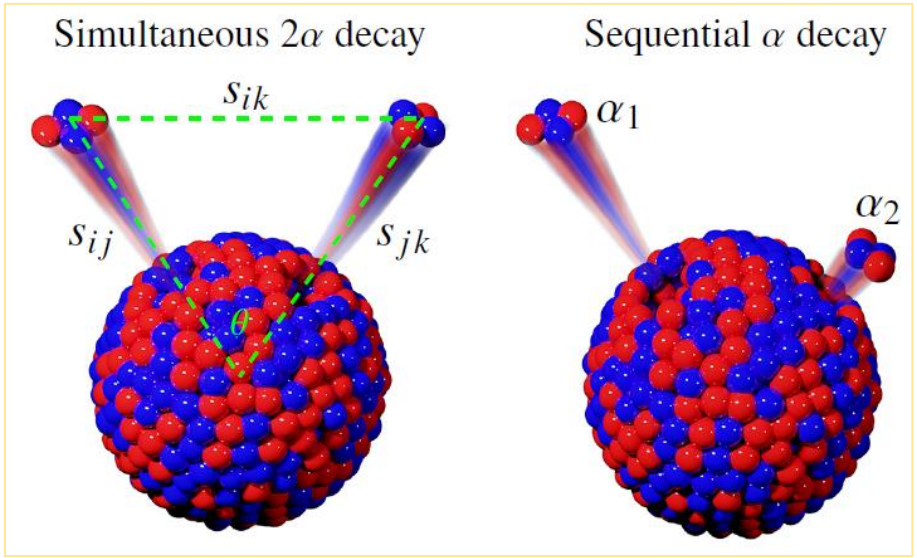
$$V(\rho,\theta) = V_N(\rho,\theta) + V_C(\rho,\theta) + \frac{\hbar^2(K+3/2)(K+5/2)}{2m\rho^2}$$

Solving the radial Schrödinger eq.

$$\left[-\frac{\hbar^2}{2\mu_\rho}\frac{d^2}{d\rho^2} + V(\rho,\theta)\right]\varphi_{nlj}(\rho;\theta) = Q_{\alpha\alpha}\varphi_{nlj}(\rho;\theta),$$

Calculating decay width:

$$\Gamma_{\alpha\alpha}(\theta) = \frac{\hbar^2 k_\rho}{\mu_\rho}\frac{\left|\varphi_{nlj}(\rho_{\mathrm{m}};\theta)\right|^2}{F_l(\eta_\rho, k_\rho\rho_{\mathrm{m}})^2 + G_l(\eta_\rho, k_\rho\rho_{\mathrm{m}})^2}$$



2. 2α decay of nuclei

Nuclear potential:

$$V_N(\rho,\theta)=\sum_{i<k}\frac{V_{ik}}{1+\exp\left[(\rho s_{ik}(\theta)-R_{ik})/a_{ik}\right]}$$

Coulomb potential:

$$V_C(\rho,\theta)=\sum_{i<k}\frac{Z_iZ_ke^2}{r_{ik}(\theta)}=\frac{1}{\rho}\sum_{i<k}\frac{Z_iZ_ke^2}{s_{ik}(\theta)}.$$

Integrating the angular distribution function:

$$\Gamma_{\alpha\alpha}=\int d\theta\, w(\theta)\,\Gamma_{\alpha\alpha}(\theta),\qquad \int d\theta w(\theta)=1.$$

$$w(\theta)=\mathcal{N}\exp\left(-\frac{(\theta-\pi)^2}{2\sigma^2}\right)$$

Branching ratio:

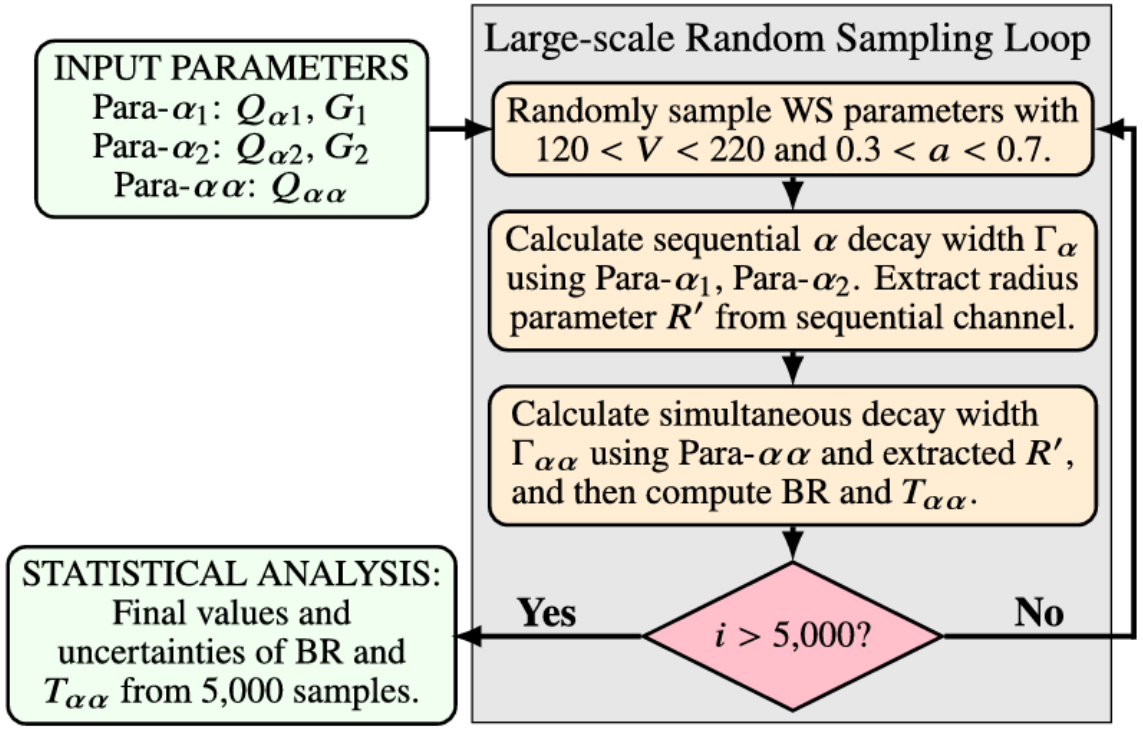
$$\mathrm{BR}=\log_{10}\left(\frac{\Gamma_{\alpha\alpha}}{\Gamma_{\alpha}}\right)$$

Resulting two-α decay half-life:

$$T_{\alpha\alpha}=\frac{\hbar\ln 2}{P_0\Gamma_{\alpha\alpha}}$$

Note: P0 = Pα1·Pα2 from CFM

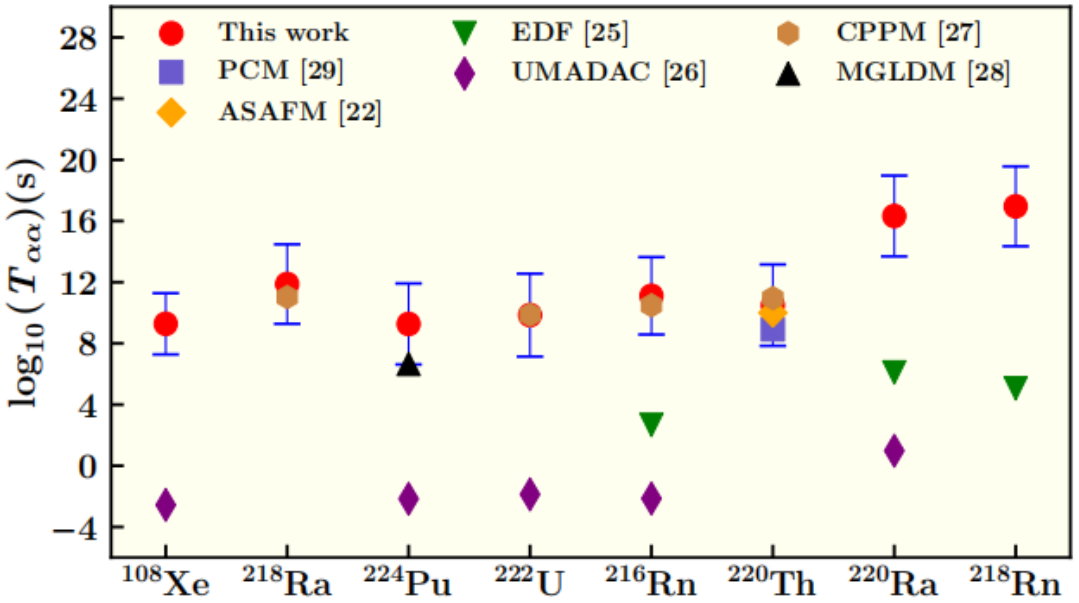
D. Deng, *et al*., J. Phys. G: Nucl. Part. Phys. 42, 075106 (2015).
D. Deng, *et al*., Rev. C 93, 044326 (2016).

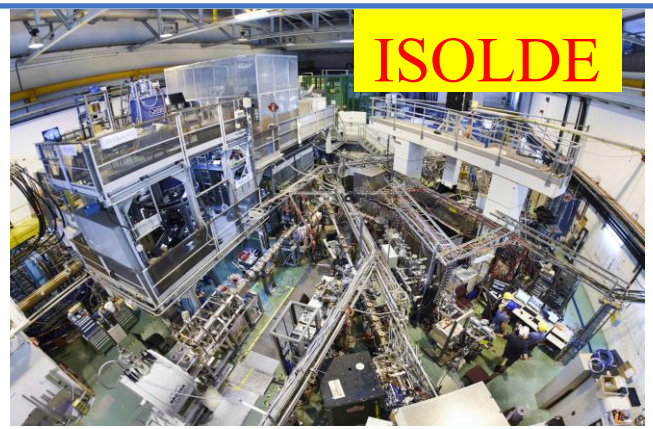


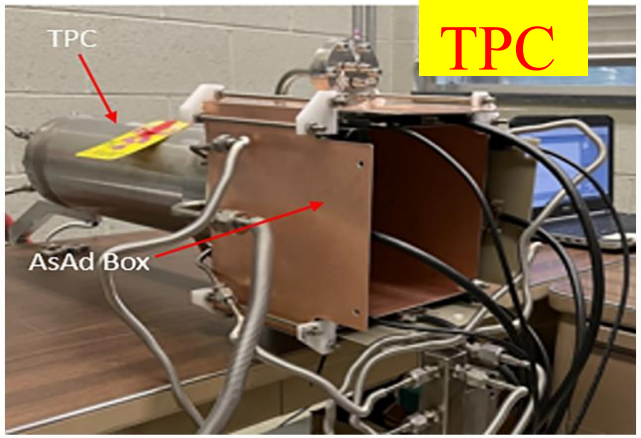
During the calculation the nuclear-potential parameters are randomly sampled to cover a sufficiently large statistical error range.

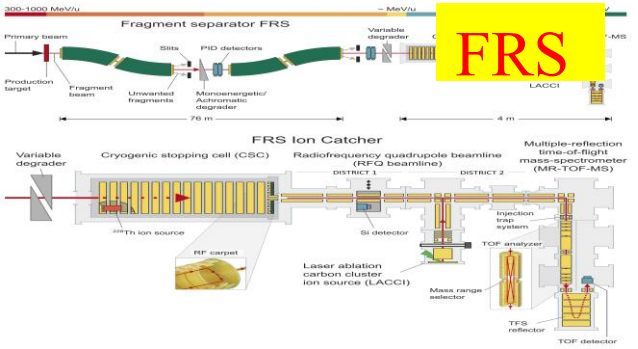
2. 2α decay of nuclei

Several experimental facilities are searching for two-α decay









The predicted lifetimes of promising two-α emitters fall within the observable range.

2. 2α decay of nuclei

南京理工大学 物理学院
SCHOOL OF PHYSICS , NANJING UNIVERSITY OF SCIENCE&TECHNOLOGY

Physical Review Letters

Highlights Recent Accepted Collections Authors Referees Editorial Policies Press About Editorial Team RSS

Three-Body Barrier Dynamics of Double-Alpha Decay in Heavy Nuclei

PDF Share

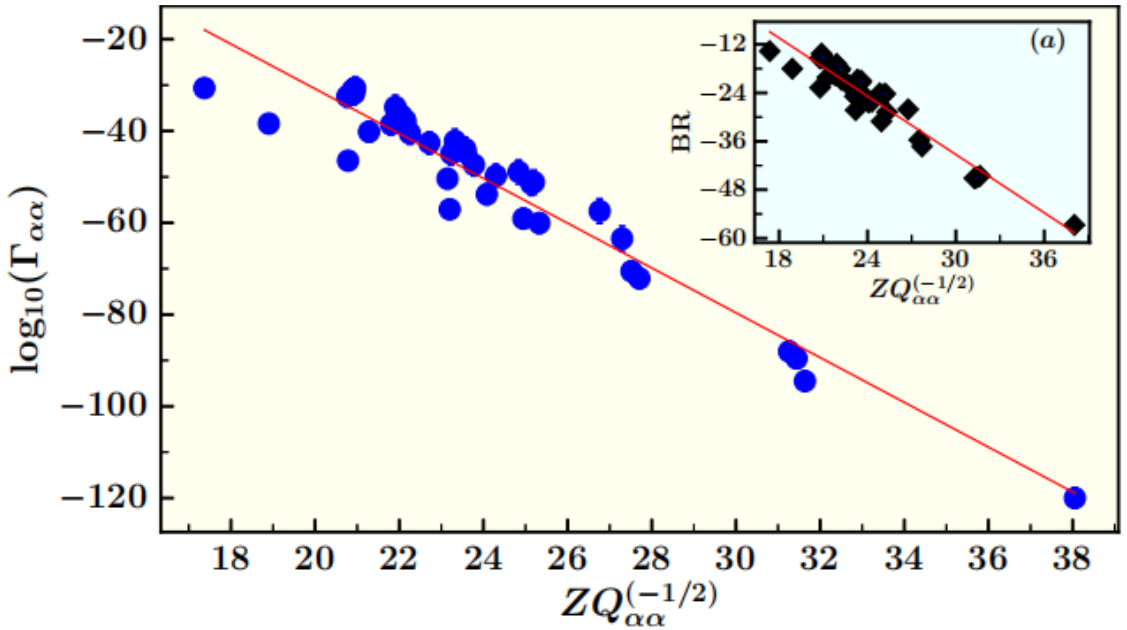
Shulin Tang [1], Tao Wan [1], Yibin Qian [1,*], Chong Qi [2], Ramon A. Wyss [2], Roberto J. Liotta [2], Dong Bai [3], Bo Zhou [4], and Zhongzhou Ren [5]

Show more

Phys. Rev. Lett. **136**, 172503 – **Published 1 May, 2026**

DOI: https://doi.org/10.1103/jxqh-6gpj

Export Citation



The two-α decay width also appears to follow a Geiger–Nuttall-like law, and its ratio to the single-α width obeys the same law

2. 2α decay of nuclei

1. Coordinate transformation: $\frac{\mathbf{r}_{ik}^2}{\rho^2} \equiv s_{ik}^2, \quad mM \equiv \sum_{i<k} m_i m_k s_{ik}^2.$

2. Taking θ = π and defining ζ as the distance between the α particle and the daughter nucleus:

$$\rho^2 = \frac{1}{m_\alpha M}\left(2m_\alpha M_{\text{core}}\zeta^2 + m_\alpha^2(2\zeta)^2\right) = \frac{2m_\alpha\zeta^2(M_{\text{core}}+2m_\alpha)}{m_\alpha(M_{\text{core}}+2m_\alpha)} = 2\zeta^2.$$

3. Total Hamiltonian:

$$H_{\text{total}} = T + V_{\text{Core}-\alpha_1}(\mathbf{r}_1) + V_{\text{Core}-\alpha_2}(\mathbf{r}_2) + V_{\alpha_1-\alpha_2}(\mathbf{r}_{12}) + V_{\text{3-body}}.$$

4. Effective Hamiltonian:

$$H_\theta^{\text{eff}} = -\frac{\hbar^2}{2\mathcal{I}}\frac{d^2}{d\theta^2} + V_{\text{eff}}(\theta), \qquad V_{\text{eff}}(\delta) \approx V_{\min} + \frac{2e^2}{\zeta}\left(1+\frac{\delta^2}{8}\right) \approx \text{const} + \frac{1}{2}\left(\frac{e^2}{2\zeta}\right)\delta^2.$$

5. Schrödinger equation:

$$\left[-\frac{\hbar^2}{2\mathcal{I}}\frac{d^2}{d\delta^2} + \frac{1}{2}k_\theta\delta^2\right]\Psi(\delta) = E\Psi(\delta).$$

6. Solution (standard form): $\Psi(\delta) \propto \exp\left(-\frac{\delta^2}{2\sigma_0^2}\right).$ **also:** $w(\theta) = |\Psi|^2$

7. Let $\sigma = \sigma_0/\sqrt{2}$ **gives:**

$$w(\theta) = \mathcal{N}\exp\left(-\frac{(\theta-\pi)^2}{2\sigma^2}\right)$$

PART 03

1. Introduction

2. α and 2α decay of nuclei

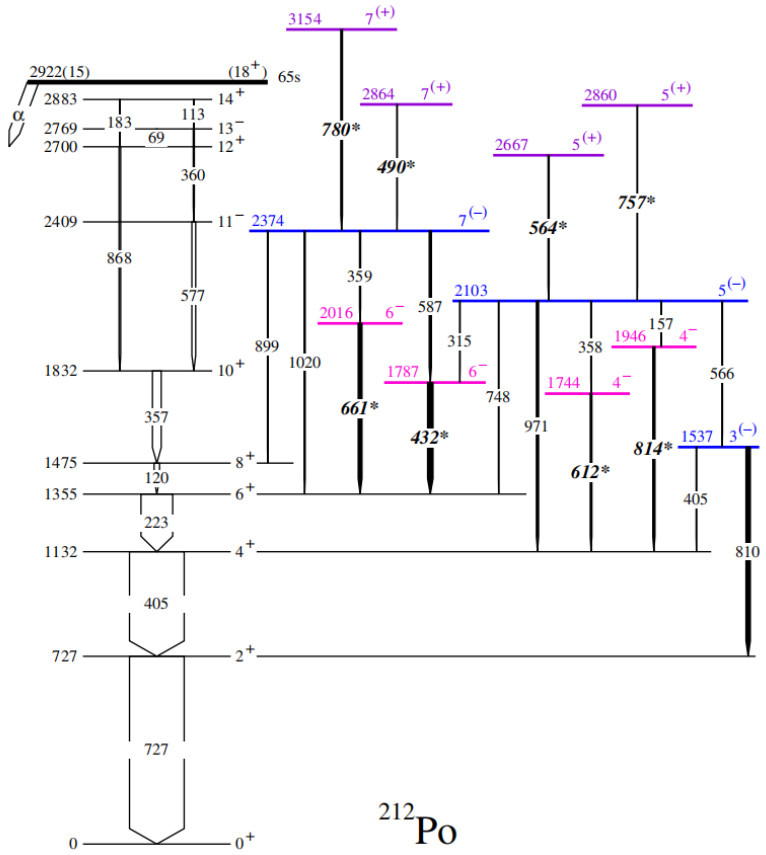
3. Cluster structure in heavy nuclei

4. Outlook

3. Cluster structure: coupled-channel method

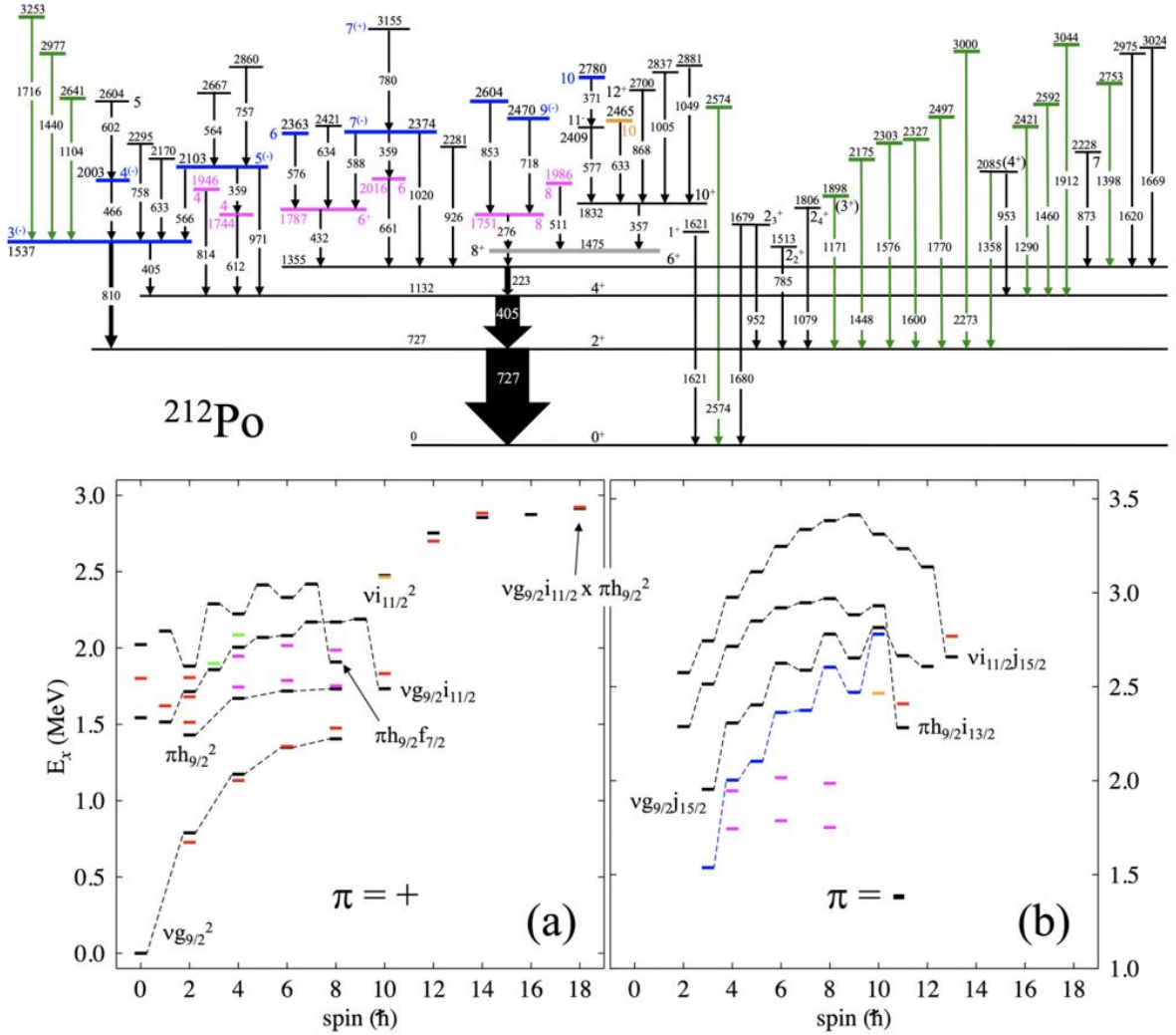
南京理工大学 物理学院
SCHOOL OF PHYSICS , NANJING UNIVERSITY OF SCIENCE&TECHNOLOGY

Non-natural-parity states of ^{212}Po



Non-natural-parity states of ^{212}Po from the ^{208}Pb(^{18}O, ^{14}C) experiment

A. Astier, et al., PRL **104**, 042701 (2010)



^{212}Po levels from ^{12}C(^{208}Pb, ^{212}Po)^{8}Be and shell-model results

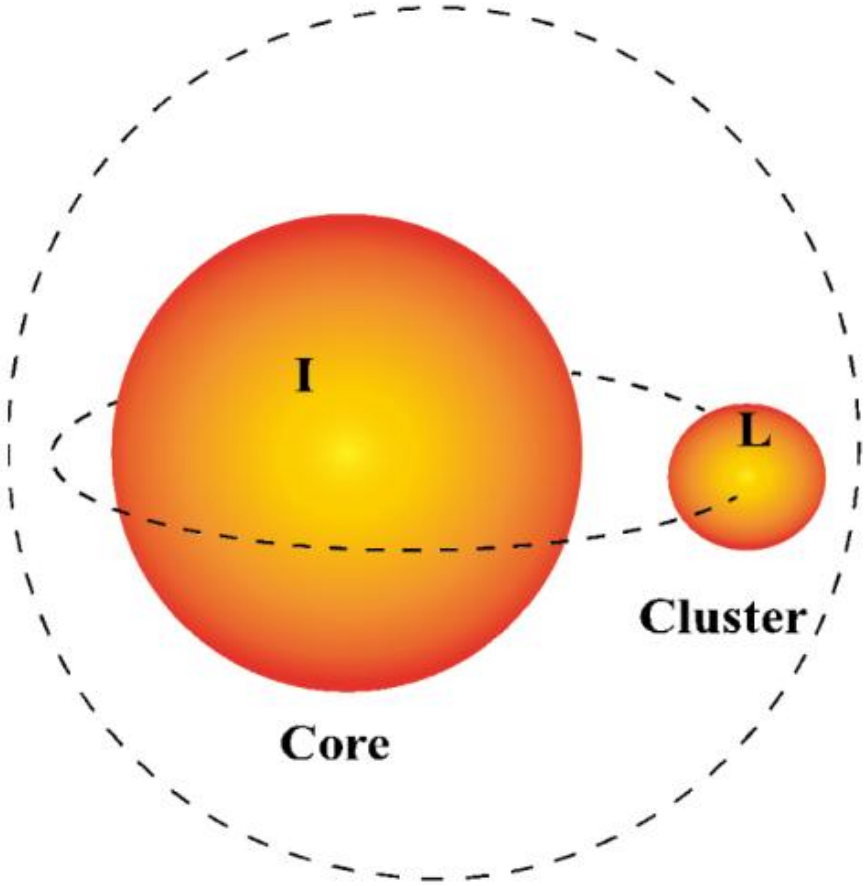
A. Fernández, et al., PRC **104**, 054316 (2021)

Positive-parity states

Shell-model multiplet

3. Cluster structure: coupled-channel method

Coupled-channel with core excitation



Physical picture of the coupled-channel method

Total $H = T + H_C + V$

$$\langle \psi_{I'L'J}|H|\psi_{ILJ}\rangle = E^J_{IL}\delta_{I,I'}\delta_{L,L'} + \sum_{l=2,3}(-1)^{l+I+L}\hat{I}\hat{I}'\hat{L}\hat{L}' \times \langle I0I'0|l0\rangle\langle L0L'0|l0\rangle W(IlJL';I'L)\beta^J_{lII'},$$

with

$$E^J_{IL} = \langle \chi^J_{IL}|T_L + V_0|\chi^J_{IL}\rangle + A_I = E(L) + A_I$$

$$\beta^J_{lII'} = (\kappa_{I'}/4\pi)\langle \chi^J_{I'L'}|V_l|\chi^J_{IL}\rangle.$$

E(L) determined from the previous two-body cluster model

AI —— A0, A3 *β —— β2, β3*

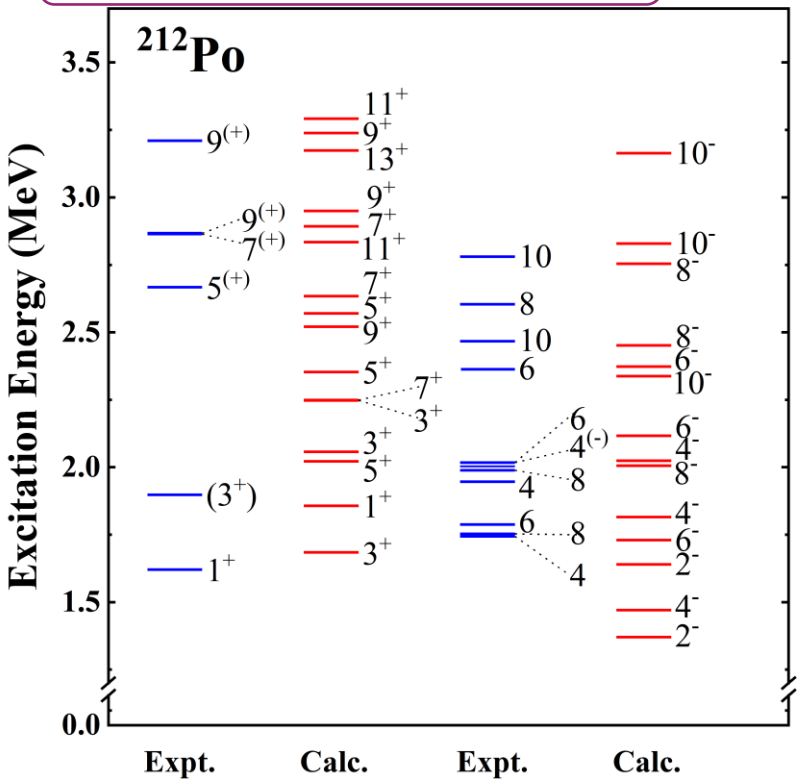
Electromagnetic transition multipole operators:

$$\langle \Psi_{J'}||r^\lambda Y_\lambda(\hat{\boldsymbol{r}})||\Psi_J\rangle = \sum_{I'L'}\sum_{IL}\delta_{I,I'}(-1)^L C^J_{IL}C^{J'}_{I'L'}\gamma_\lambda\sqrt{\frac{1}{4\pi}}\hat{J}\hat{J}'\hat{L}\hat{L}' \times W(ILJ'\lambda;JL')\langle L0L'0|\lambda0\rangle\langle \chi^{J'}_{I'L'}|r^\lambda|\chi^J_{IL}\rangle,$$

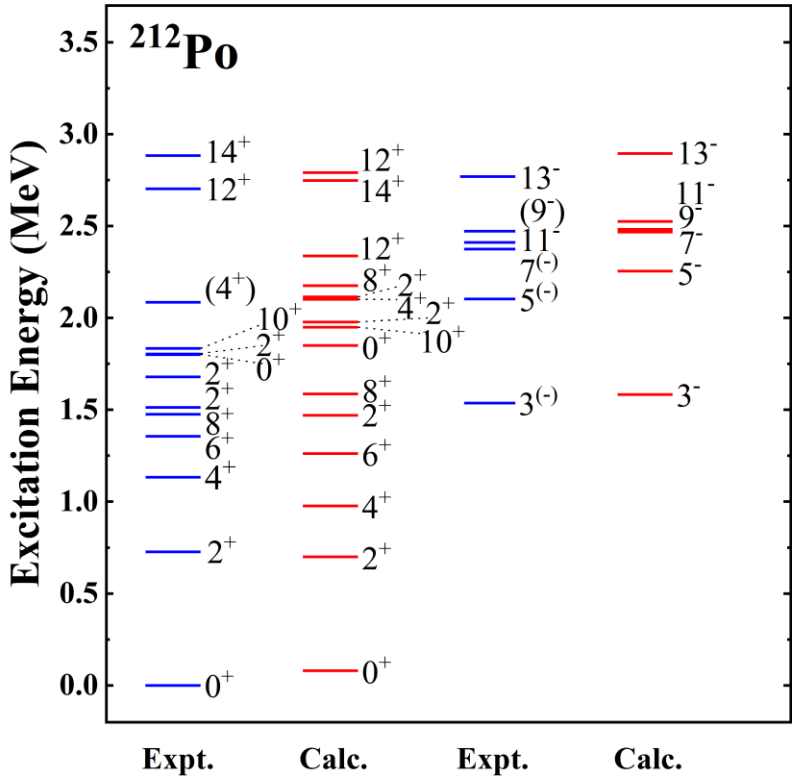
3. Cluster structure: coupled-channel method

南京理工大学 物理学院
SCHOOL OF PHYSICS , NANJING UNIVERSITY OF SCIENCE&TECHNOLOGY

Levels of ^{212}Po and ^{216}Rn

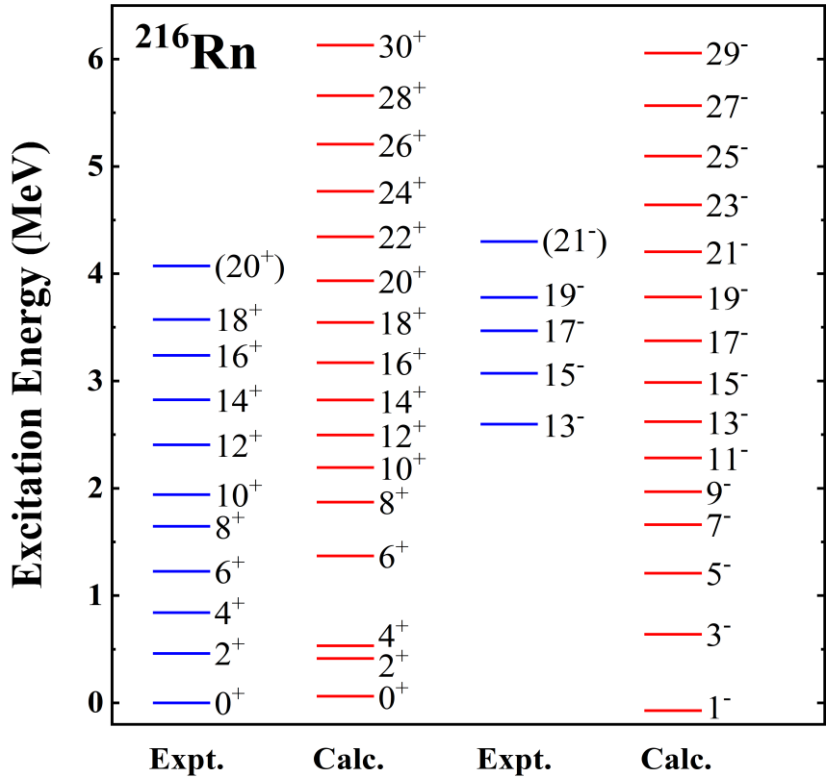


Non-natural-parity levels



Natural-parity levels

^{212}Po (α + ^{208}Pb)



Parity doublet

^{216}Rn (^{8}Be + ^{208}Pb)

Reproduction of the level structure confirms the reliability of the coupled-channel method

Tao Wan, Yibin Qian, PRC **112**, 034336 (2025)

3. Cluster structure: coupled-channel method

南京理工大学物理学院
SCHOOL OF PHYSICS , NANJING UNIVERSITY OF SCIENCE&TECHNOLOGY

E1/E2 transitions in ^{212}Po and ^{216}Rn

Calculated B(E2) values of ^{212}Po

$J_i^\pi \to J_f^\pi$	$B(E2)_{\text{expt.}}$	$B(E2)_{\text{calc.}}$	$B(E2)_{\text{I}}$
$2_1^+ \to 0^+$	$2.57^{+0.38}_{-0.29}$	33.07	4.51
$4^+ \to 2^+$	$9.40^{+1.30}_{-1.30}$	7.33	0.27
$6^+ \to 4^+$	$13.20^{+4.90}_{-2.90}/3.90^{+1.10}_{-1.10}$	3.98	2.40
$8^+ \to 6^+$	$4.56^{+0.12}_{-0.12}/2.30^{+0.09}_{-0.09}$	2.93	4.67
$10^+ \to 8^+$	$2.20^{+0.80}_{-0.40}$	1.98	5.60
$2_2^+ \to 0^+$	$0.39^{+0.06}_{-0.06}$	2.06	
$2_2^+ \to 2_1^+$	$0.32^{+0.26}_{-0.18}$	1.07	
$2_3^+ \to 0^+$	$0.27^{+0.07}_{-0.07}$	1.03	
$2_3^+ \to 2_1^+$	$3.90^{+3.70}_{-2.90}$	0.87	

M. von Tresckow, et al., PLB **821**, 136624 (2021)
Y. Suzuki, et al., PRC **82**, 041303(R) (2010)
M. E. Debray, et al., PRC **73**, 024314 (2006)

These results further suggest the presence of cluster structure in heavy nuclei and confirm the reliability of the coupled-channel method

Calculated B(E1) values

^{212}Po			^{216}Rn		
J_i^π	$B(E1)_{\text{calc.}}$	$B(E1)_{\text{expt.}}$	J_i^π	$B(E1)_{\text{calc.}}$	$B(E1)_{\text{II}}$
2_1^-	1.748		1^-	2516.505	150.831
2_2^-	0.010		3^-	107.216	142.212
4_1^-	1.751	$2.5^{+1.1}_{-0.6}$	5^-	327.638	129.284
4_2^-	0.079		7^-	4.751	9.912
4_3^-	0.035		9^-	4.385	24.564
6_1^-	0.123	$7.5^{+1.7}_{-1.2}$	11^-	4.235	1.034
6_2^-	0.001		13^-	1.486	0.047
6_3^-	0.001		15^-	0.305	64.642
8_1^-	0.060	$26.0^{+11.0}_{-8.0}$	17^-	0.014	112.046
8_2^-	0.002		19^-	0.025	0.147
8_3^-	0.0004		14^+	0.367	0.362

B. D. C. Kimene Kaya, et al., PRC **105**, 034327 (2022)

B(E1)/B(E2) ratio of ^{216}Rn

J_i^π	Expt.	Present	Ref
15^-	0.70(10)	1.75	213.00
16^+	0.13(3)	0.10	213.00
17^-	0.60(10)	0.09	383.00
19^-	0.05(2)	0.18	0.66

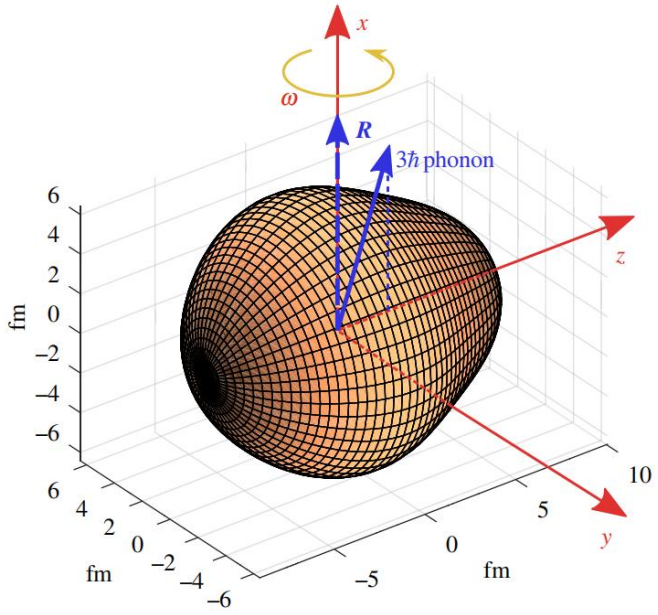
B. D. C. Kimene Kaya, et al., PRC **105**, 034327 (2022)

Tao Wan, Yibin Qian, PRC **112**, 034336 (2025)

3. Cluster structure: coupled-channel method

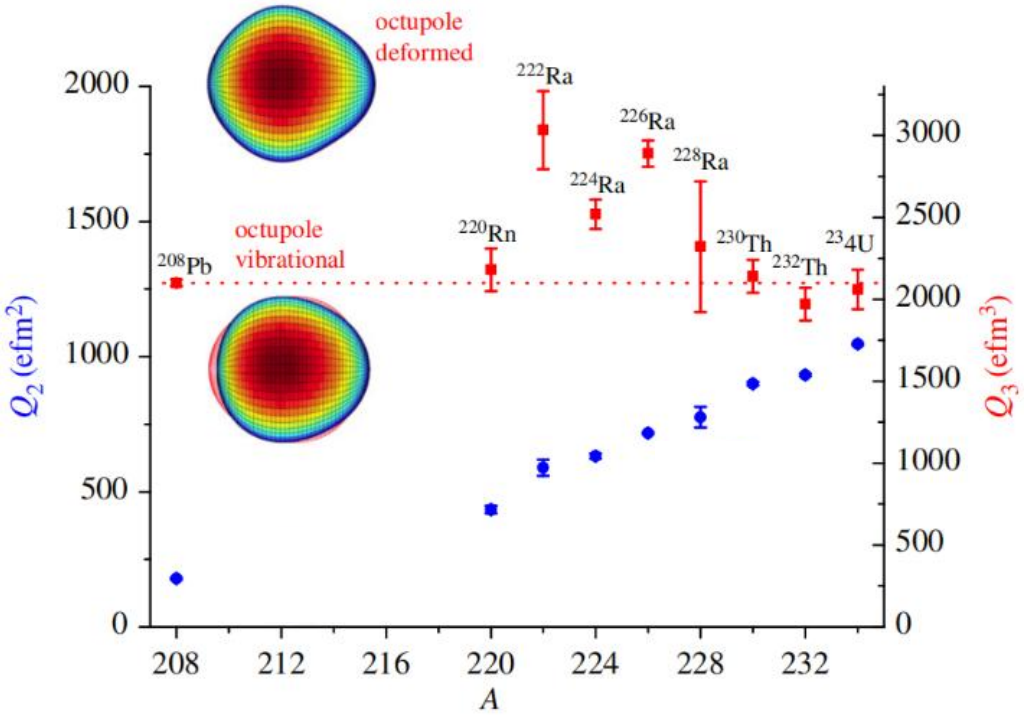
南京理工大学 物理学院
SCHOOL OF PHYSICS , NANJING UNIVERSITY OF SCIENCE&TECHNOLOGY

Octupole deformation in the Ra isotope chain



Pear-shaped nucleus

Fermi-surface nucleons occupy orbitals of opposite parity with $\Delta l = \Delta j = 3\hbar$, giving strong octupole correlations



E2 and E3 intrinsic moments Qλ

P.A. Butler, et al., Nat. Commun. **10**, 2473 (2019)
P. A. Butler, J. Phys. G **43**, 073002 (2016).

Signatures: octupole magic numbers, pear-shaped asymmetry, alternating parities, enhanced E1/E3 strengths

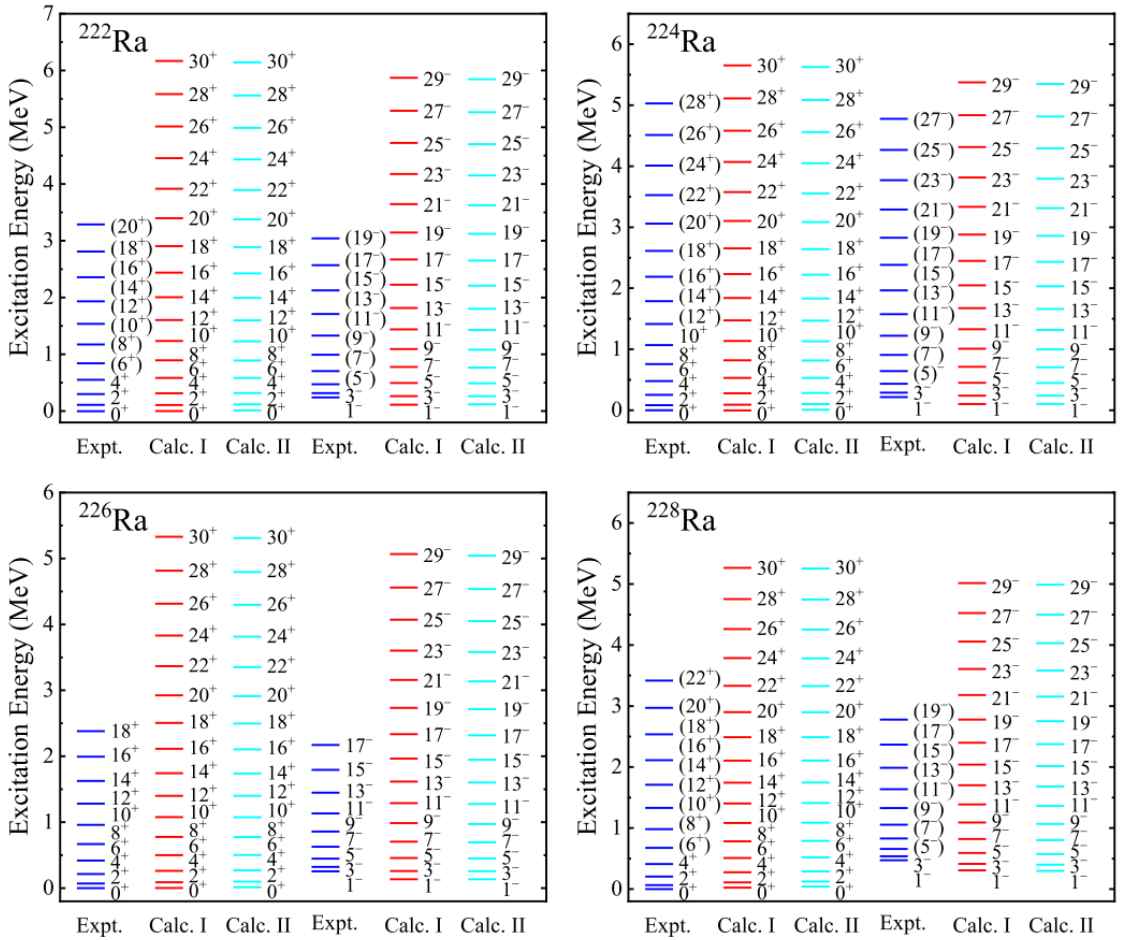
Theory: breaking of spatial-reflection symmetry, very large model spaces required, and an ambiguous separation between static and dynamic octupole deformation

Experiment: target nuclides are extremely hard to produce (too short-lived) and E3 decay branchings are very low

3. Cluster structure: coupled-channel method

南京理工大学 物理学院
SCHOOL OF PHYSICS , NANJING UNIVERSITY OF SCIENCE&TECHNOLOGY

Octupole deformation in the Ra isotope chain



^{222}Ra (^{14}C + ^{208}Pb)
^{226}Ra (^{18}C + ^{208}Pb)
Calc. I: 0^+, octupole 3^- state

^{224}Ra (^{16}C + ^{208}Pb)
^{228}Ra (^{20}C + ^{208}Pb)
Calc. II: 0^+, octupole 3^- state, quadrupole 2^+ state

Reduced E2/E3 matrix elements

	^{222}Ra (efm$^\lambda$)			^{224}Ra (efm$^\lambda$)		
$\lvert\langle J_f\lvert\lvert M(E\lambda)\rvert\rvert J_i\rangle\rvert$	Expt.	Calc. I	Calc. II	Expt.	Calc. I	Calc. II
$\lvert\langle 0^+\lvert\lvert M(E2)\rvert\rvert 2^+\rangle\rvert$	211±60	172	174	199±3	173	175
$\lvert\langle 2^+\lvert\lvert M(E2)\rvert\rvert 4^+\rangle\rvert$	298±15	368	372	315±6	370	375
$\lvert\langle 4^+\lvert\lvert M(E2)\rvert\rvert 6^+\rangle\rvert$	357±18	555	561	405±15	559	565
$\lvert\langle 6^+\lvert\lvert M(E2)\rvert\rvert 8^+\rangle\rvert$	415±23	739	747	500±60	744	753
$\lvert\langle 1^-\lvert\lvert M(E2)\rvert\rvert 3^-\rangle\rvert$	235±22	269	272	230±11	271	274
$\lvert\langle 3^-\lvert\lvert M(E2)\rvert\rvert 5^-\rangle\rvert$	310±40	450	453	410±60	459	463
$\lvert\langle 0^+\lvert\lvert M(E3)\rvert\rvert 3^-\rangle\rvert$	1130±90	1045	1064	940±30	1026	1045
$\lvert\langle 2^+\lvert\lvert M(E3)\rvert\rvert 1^-\rangle\rvert$	850±240	783	798	1370±140	767	782
$\lvert\langle 2^+\lvert\lvert M(E3)\rvert\rvert 3^-\rangle\rvert$	900±500	1206	1228	<4000	1184	1206
$\lvert\langle 2^+\lvert\lvert M(E3)\rvert\rvert 5^-\rangle\rvert$	1790±200	1995	2030	1410±190	1964	1999

	^{226}Ra (efm$^\lambda$)			^{228}Ra (efm$^\lambda$)		
$\lvert\langle J_f\lvert\lvert M(E\lambda)\rvert\rvert J_i\rangle\rvert$	Expt.	Calc. I	Calc. II	Expt.	Calc. I	Calc. II
$\lvert\langle 0^+\lvert\lvert M(E2)\rvert\rvert 2^+\rangle\rvert$	226±1	175	177	242±50	177	180
$\lvert\langle 2^+\lvert\lvert M(E2)\rvert\rvert 4^+\rangle\rvert$	370^{+9}_{-5}	374	379	387±19	381	387
$\lvert\langle 4^+\lvert\lvert M(E2)\rvert\rvert 6^+\rangle\rvert$	483^{+6}_{-7}	565	572	511±26	577	585
$\lvert\langle 6^+\lvert\lvert M(E2)\rvert\rvert 8^+\rangle\rvert$	541^{+7}_{-10}	754	763	589±29	770	781
$\lvert\langle 1^-\lvert\lvert M(E2)\rvert\rvert 3^-\rangle\rvert$	366^{+6}_{-12}	272	275	380±50	269	271
$\lvert\langle 3^-\lvert\lvert M(E2)\rvert\rvert 5^-\rangle\rvert$	409^{+5}_{-10}	461	465	390^{+40}_{-80}	453	457
$\lvert\langle 0^+\lvert\lvert M(E3)\rvert\rvert 3^-\rangle\rvert$	1080±30	1001	1019	870±150	939	955
$\lvert\langle 2^+\lvert\lvert M(E3)\rvert\rvert 1^-\rangle\rvert$	1190^{+30}_{-70}	749	764	1360±230	714	697
$\lvert\langle 2^+\lvert\lvert M(E3)\rvert\rvert 3^-\rangle\rvert$	1150±160	1156	1178	60^{+160}_{-230}	1087	1105
$\lvert\langle 2^+\lvert\lvert M(E3)\rvert\rvert 5^-\rangle\rvert$	2000±70	2064	1656	1710±230	1765	1796

L. P. Gaffney, et al., Nature **497**, 199 (2013)
H. J. Wollersheim, et al., NPA **556**, 261 (1993)
P. A. Butler, et al., PRL **124**, 042503 (2020)

Tao Wan, Yibin Qian, PRC **113**, 034313 (2026)

3. Cluster structure: coupled-channel method

南京理工大学 物理学院
SCHOOL OF PHYSICS , NANJING UNIVERSITY OF SCIENCE&TECHNOLOGY

Octupole deformation in the Ra isotope chain

Reduced matrix elements of the E1 transition

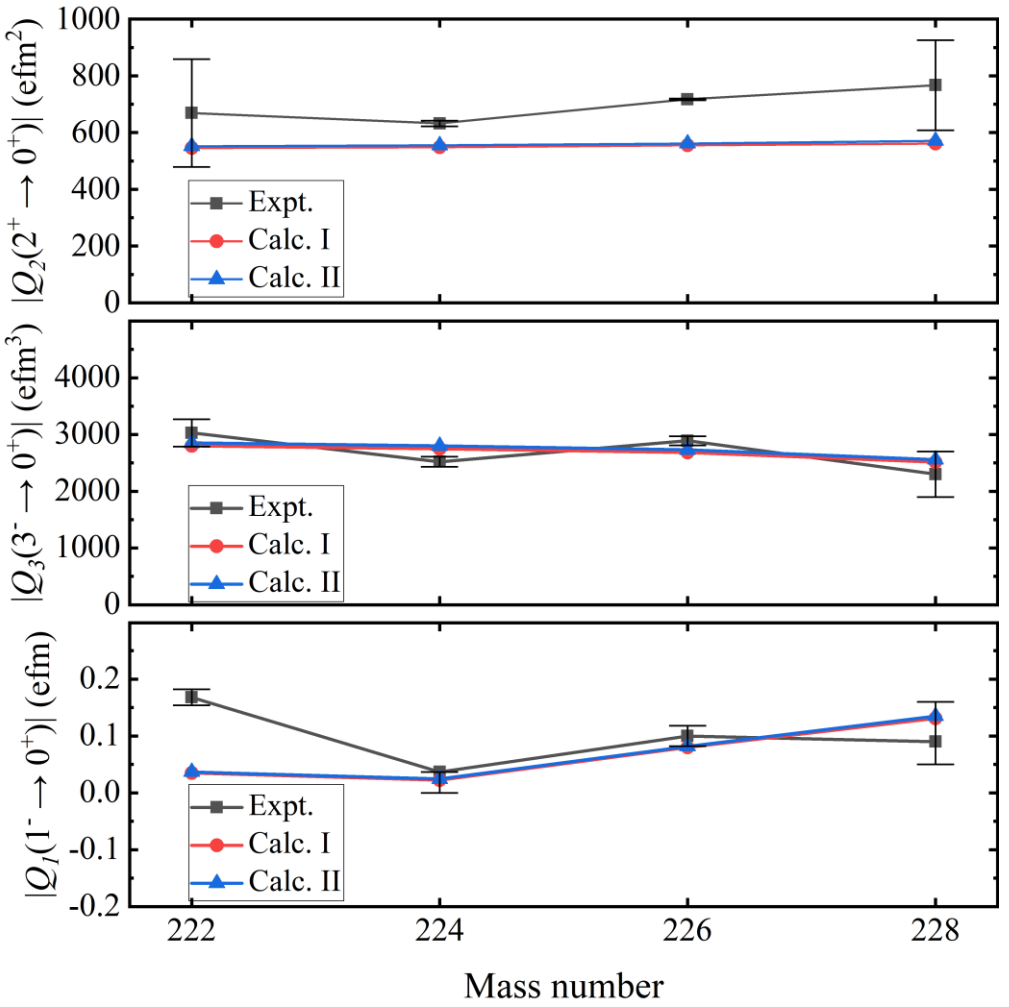
$\lvert\langle J_f\lvert\lvert M(E\lambda)\rvert\rvert J_i\rangle\rvert$	^{222}Ra (efm$^\lambda$)			^{224}Ra (efm$^\lambda$)		
	Expt	Calc. I	Calc. II	Expt	Calc. I	Calc. II
$\lvert\langle 0^+\lvert\lvert M(E1)\rvert\rvert 1^-\rangle\rvert$	0.082 ± 0.007	0.017	0.018	< 0.018	0.011	0.012
$\lvert\langle 2^+\lvert\lvert M(E1)\rvert\rvert 3^-\rangle\rvert$	0.26 ± 0.05	0.045	0.047	0.026 ± 0.005	0.029	0.030
$\lvert\langle 4^+\lvert\lvert M(E1)\rvert\rvert 5^-\rangle\rvert$	$0.18^{+0.048}_{-0.019}$	0.073	0.076	0.030 ± 0.010	0.046	0.048
$\lvert\langle 5^-\lvert\lvert M(E1)\rvert\rvert 6^+\rangle\rvert$	0.277 ± 0.011	0.087	0.091		0.055	0.057
$\lvert\langle 7^-\lvert\lvert M(E1)\rvert\rvert 8^+\rangle\rvert$	0.317 ± 0.018	0.114	0.119		0.073	0.076
$\lvert\langle 8^+\lvert\lvert M(E1)\rvert\rvert 9^-\rangle\rvert$	0.48 ± 0.04	0.127	0.133		0.081	0.085
$\lvert\langle 2^+\lvert\lvert M(E1)\rvert\rvert 1^-\rangle\rvert$	$0.114^{+0.025}_{-0.009}$	0.024	0.025	< 0.03	0.015	0.016
$\lvert\langle 4^+\lvert\lvert M(E1)\rvert\rvert 3^-\rangle\rvert$	0.27 ± 0.26	0.052	0.054		0.033	0.034

$\lvert\langle J_f\lvert\lvert M(E\lambda)\rvert\rvert J_i\rangle\rvert$	^{226}Ra (efm$^\lambda$)			^{228}Ra (efm$^\lambda$)		
	Expt	Calc. I	Calc. II	Expt	Calc. I	Calc. II
$\lvert\langle 0^+\lvert\lvert M(E1)\rvert\rvert 1^-\rangle\rvert$	0.050 ± 0.009	0.039	0.040	$0.043^{+0.032}_{-0.020}$	0.064	0.066
$\lvert\langle 2^+\lvert\lvert M(E1)\rvert\rvert 3^-\rangle\rvert$	0.061 ± 0.007	0.101	0.105	0.09 ± 0.04	0.167	0.172
$\lvert\langle 4^+\lvert\lvert M(E1)\rvert\rvert 5^-\rangle\rvert$	0.093 ± 0.007	0.163	0.169	0.13 ± 0.06	0.264	0.273
$\lvert\langle 5^-\lvert\lvert M(E1)\rvert\rvert 6^+\rangle\rvert$		0.195	0.202	$0.074^{+0.018}_{-0.012}$	0.317	0.328
$\lvert\langle 7^-\lvert\lvert M(E1)\rvert\rvert 8^+\rangle\rvert$	0.21 ± 0.08	0.256	0.266	$0.13^{+0.10}_{-0.33}$	0.410	0.426
$\lvert\langle 8^+\lvert\lvert M(E1)\rvert\rvert 9^-\rangle\rvert$	0.24 ± 0.02	0.286	0.297	$0.20^{+0.20}_{-0.09}$	0.450	0.469
$\lvert\langle 2^+\lvert\lvert M(E1)\rvert\rvert 1^-\rangle\rvert$		0.055	0.056	$0.051^{+0.033}_{-0.022}$	0.091	0.093
$\lvert\langle 4^+\lvert\lvert M(E1)\rvert\rvert 3^-\rangle\rvert$		0.117	0.121	$0.080^{+0.036}_{-0.023}$	0.194	0.200

L. P. Gaffney, et al., Nature **497**, 199 (2013)
H. J. Wollersheim, et al., NPA **556**, 261 (1993)
P. A. Butler, et al., PRL **124**, 042503 (2020)

Intrinsic moments:

$$Q_\lambda = \frac{\langle J_f||M(E\lambda)||J_i\rangle}{\sqrt{(2J_f+1)(2\lambda+1)/16\pi}\,\langle J_f 0\lambda 0|J_i\rangle}$$



Tao Wan, Yibin Qian, PRC **113**, 034313 (2026)

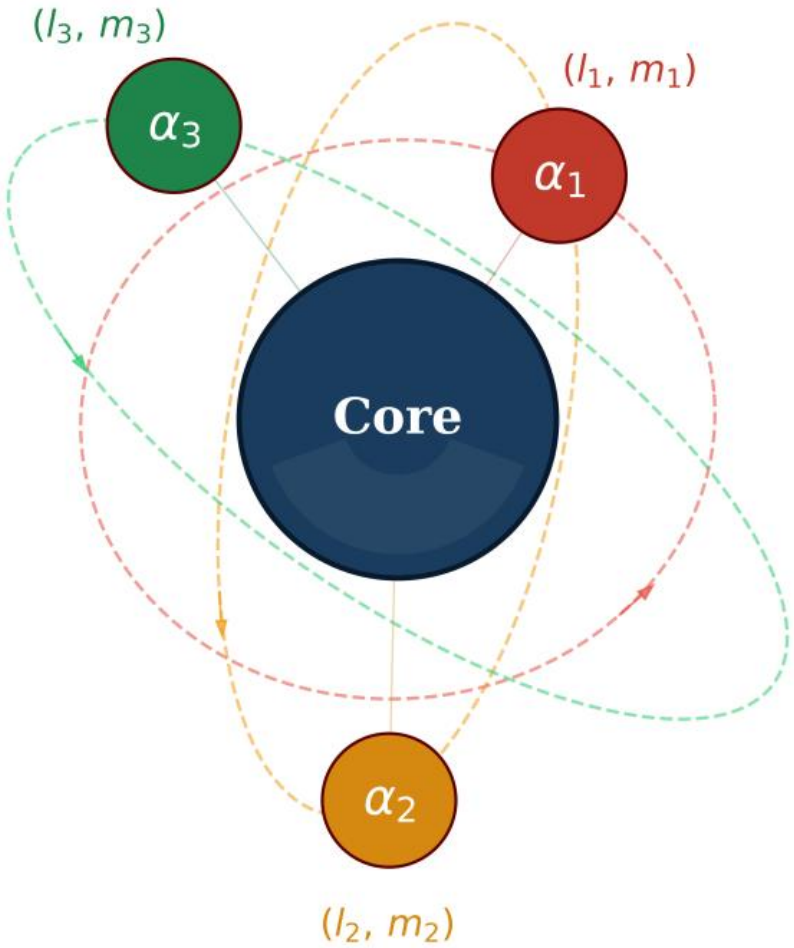
3. Cluster structure: interacting α-boson model

南京理工大学 物理学院
SCHOOL OF PHYSICS , NANJING UNIVERSITY OF SCIENCE&TECHNOLOGY

α-IBM theoretical framework

α-like bosons: stable, with zero spin and zero isospin

Example: $^{220}\mathrm{Ra} \longrightarrow {}^{208}\mathrm{Pb} + \alpha + \alpha + \alpha$



Coupling basis vectors pairwise: low computational efficiency

$$|[(l_1 l_2)L_{12}, l_3]LM\rangle = \sum_{l_1 m_1, l_2 m_2, l_3 m_3} \left(\sum_{M_{12}} C^{L_{12} M_{12}}_{l_1 m_1, l_2 m_2} C^{LM}_{L_{12} M_{12}, l_3 m_3} \right) |l_1 m_1\rangle |l_2 m_2\rangle |l_3 m_3\rangle$$

Uncoupled basis vectors: direct-product representation (M-scheme)

$$|LM\rangle = \sum_{l_1 m_1, l_2 m_2, l_3 m_3} C_{l_1 m_1, l_2 m_2, l_3 m_3} |l_1 m_1\rangle |l_2 m_2\rangle |l_3 m_3\rangle$$

$$H = \lambda_{sp} H_{sp} + \lambda_{L^2} \hat{L}^2 + \lambda_{QQ} \hat{Q} \cdot \hat{Q} + \lambda_{OO} \hat{O} \cdot \hat{O}$$

Hsp: single-particle energy (α–core coupling, from the BCM);

$\hat{L}^2$ angular-momentum-squared term, rotational band L(L+1);

$$\mathbf{L}^2 = \sum_{i=1}^{3} \mathbf{L}_i^2 + 2 \sum_{i<j} \mathbf{L}_i \cdot \mathbf{L}_j .$$

$$\mathbf{L}_i \cdot \mathbf{L}_j = L_{i,z} L_{j,z} + \frac{1}{2} \left(L_{i,+} L_{j,-} + L_{i,-} L_{j,+} \right) .$$

Diagonal: $$\langle m_1, m_2, m_3 | \mathbf{L}^2 | m_1, m_2, m_3 \rangle = \sum_{i=1}^{3} l_i (l_i + 1) + 2 \sum_{i<j} m_i m_j .$$

Off-diagonal: $$\langle m_1 + 1, m_2 - 1, m_3 | L_{1,+} L_{2,-} | m_1, m_2, m_3 \rangle$$

$$= \sqrt{[l_1(l_1+1) - m_1(m_1+1)]\,[l_2(l_2+1) - m_2(m_2-1)]}$$

3. Cluster structure: interacting α-boson model

α-IBM framework

$\hat{Q}\cdot\hat{Q}$: quadrupole interaction → ellipsoidal deformation;

$$\hat{Q}\cdot\hat{Q} = -\lambda_{QQ}\sum_{\mu} Q_{2\mu}(1)Q_{2,-\mu}(2)$$

单粒子四极算符：$Q_{2\mu} = r^2 Y_{2\mu}(r)$

$$\langle n_\alpha l_\alpha m_\alpha | Q_{2\mu} | n_\gamma l_\gamma m_\gamma \rangle = R^{(2)}_{\alpha\gamma}(-1)^{-m_\alpha}\begin{pmatrix} l_\alpha & 2 & l_\gamma \\ -m_\alpha & \mu & m_\gamma \end{pmatrix}$$

$$\times\sqrt{\frac{2(l_\alpha+1)5(2l_\gamma+1)}{4\pi}}\begin{pmatrix} l_\alpha & 2 & l_\gamma \\ 0 & 0 & 0 \end{pmatrix}$$

二次量子化下：$Q^{\alpha\gamma}_{2\mu} = \langle \alpha | Q_{2\mu} | \gamma \rangle$

两体矩阵元：$V_{\alpha\beta,\gamma\delta} = -\sum_{\mu}(-1)^{\mu} Q^{\alpha\gamma}_{2\mu} Q^{\beta\delta}_{2,-\mu}$

$$\hat{Q}\cdot\hat{Q} = \frac{1}{2}\sum_{\alpha\beta\gamma\delta} V_{\alpha\beta,\gamma\delta} a^{+}_{\alpha} a^{+}_{\beta} a_{\delta} a_{\gamma}$$

$$_S\langle N_i | \hat{V}_{QQ} | N_j \rangle_S = \frac{1}{2}\sum_{\alpha\beta\gamma\delta} V_{\alpha\beta,\gamma\delta\,S}\langle N_i | a^{\dagger}_{\alpha} a^{\dagger}_{\beta} a_{\delta} a_{\gamma} | N_j \rangle_S$$

$\hat{O}\cdot\hat{O}$: breaks spatial-inversion symmetry, driving the system towards a pear-shaped deformation

电磁多极算符：$T_{\lambda\mu} = \sum_{i=1}^{N} r^{\lambda} Y_{\lambda\mu}(r)$

二次量子化形式：$T_{\lambda\mu} = \sum_{\alpha\beta} t^{\alpha\beta}_{\lambda\mu} a^{+}_{\alpha} a_{\beta}$

单粒子矩阵元：$t^{\alpha\beta}_{\lambda\mu} = \langle n_\alpha l_\alpha m_\alpha | r^{\lambda} Y_{\lambda\mu}(r) | n_\beta l_\beta m_\beta \rangle$

m－scheme矩阵元：

$$M^{(m)}_{\beta\mu\alpha} = \langle n_\beta l_\beta m_\beta | T_{\lambda\mu} | n_\alpha l_\alpha m_\alpha \rangle = (-1)^{l_\beta - m_\beta}\begin{pmatrix} l_\beta & \lambda & l_\alpha \\ -m_\alpha & \mu & m_\alpha \end{pmatrix}\langle n_\beta l_\beta | T_\lambda | n_\alpha l_\alpha \rangle$$

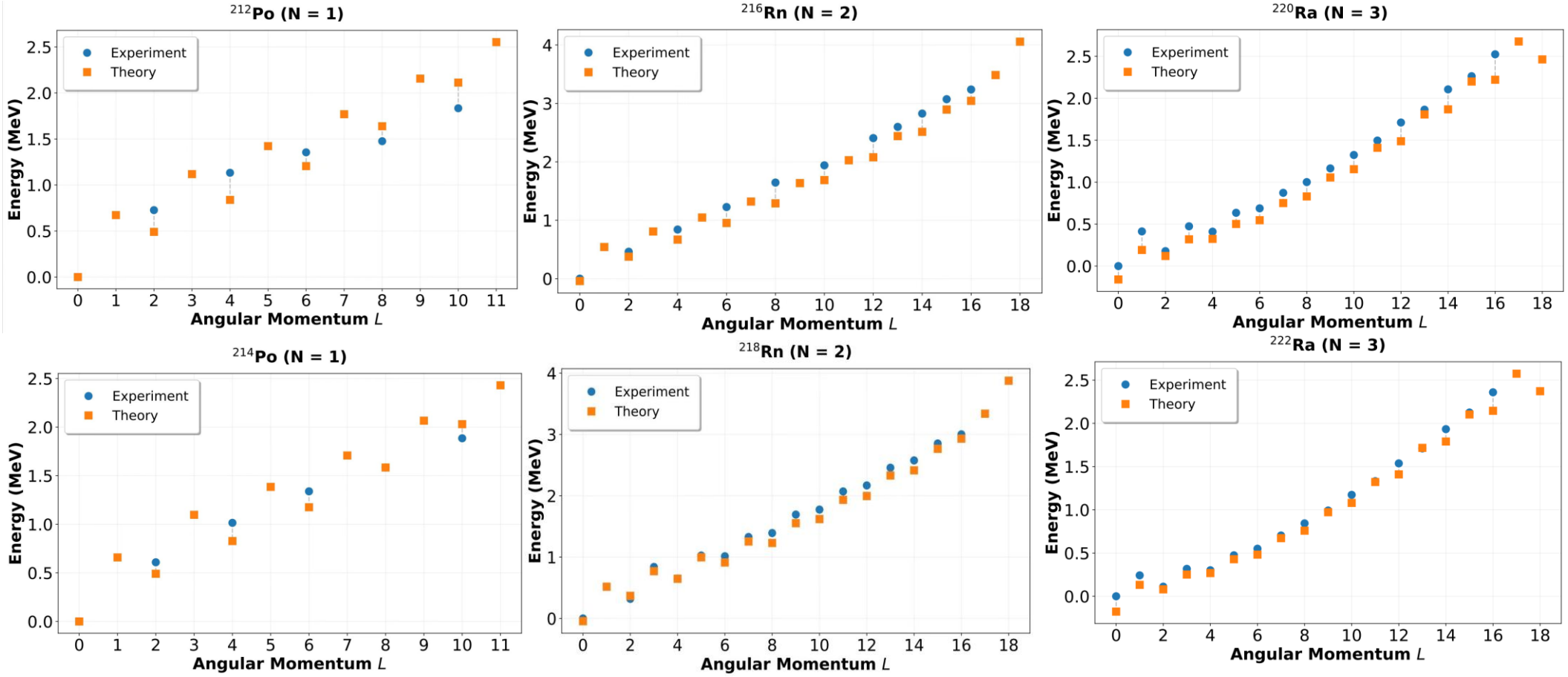
因此：$B(E\lambda;\alpha\to\beta) = \frac{1}{2l_\alpha+1}\frac{\left|M^{(m)}_{\beta\mu\alpha}\right|^2}{\begin{pmatrix} l_\beta & \lambda & l_\alpha \\ -m_\beta & \mu & m_\alpha \end{pmatrix}^2}$

3. Cluster structure: interacting α-boson model

南京理工大学 物理学院
SCHOOL OF PHYSICS , NANJING UNIVERSITY OF SCIENCE&TECHNOLOGY

Structural evolution in the α-IBM framework

Preliminary Results



^{220}Ra → ^{216}Rn → ^{212}Po

^{222}Ra → ^{218}Rn → ^{214}Po

Summary

- Cluster effects inside heavy nuclei: α decay and cluster structure

- α and 2α decay of nuclei

- Possible cluster structure in heavy nuclei

✓Parity doublets in even–even nuclei

✓Spin–orbit coupling in odd-A nuclei

✓Coupling between cluster states and intrinsic degrees of freedom

α-boson framework for cluster structure

南京理工大学 物理学院
SCHOOL OF PHYSICS，NANJING UNIVERSITY OF SCIENCE&TECHNOLOGY

In collaboration with

ZZ Ren, Tongji University,

C Xu, Nanjing University,

B Zhou, Fudan University,

D Bai, Hohai University,

C Qi, R. Wyss, R. Liotta, KTH

Wei Liu,Tao Wan, Shuling Tang, Huaxuan Pan, Junyao Kong, Junjun Cai, Nanjing University of Science and Technology



谢谢！

2. α decay of nuclei: nuclear structure

南京理工大学 物理学院
SCHOOL OF PHYSICS , NANJING UNIVERSITY OF SCIENCE&TECHNOLOGY

The nuclear and Coulomb potentials between the cluster and the daughter nucleus are constructed in the double-folding model:

$$V_{N,C}(R,\beta) = \iint dr_1\, dr_2\, \rho_1(r_1)\, v(s = |R - r_1 - r_2|)\, \rho_2(r_2)$$

The total potential of the α-core system is the sum of the attractive nuclear part and the repulsive Coulomb part:

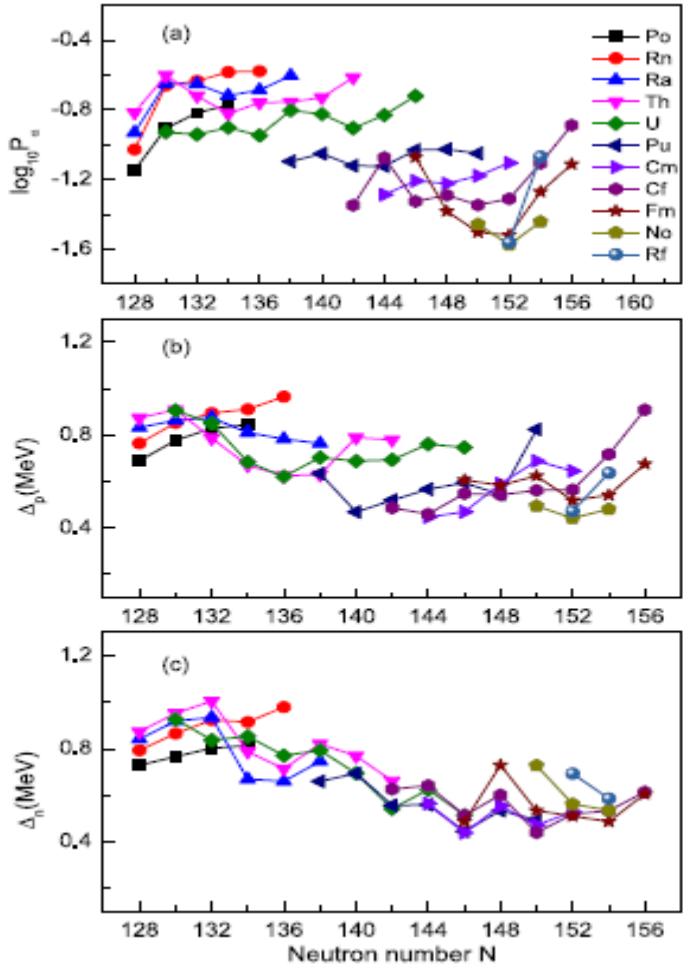
$$V(R,\beta) = \lambda V_N(R,\beta) + V_C(R,\beta)$$

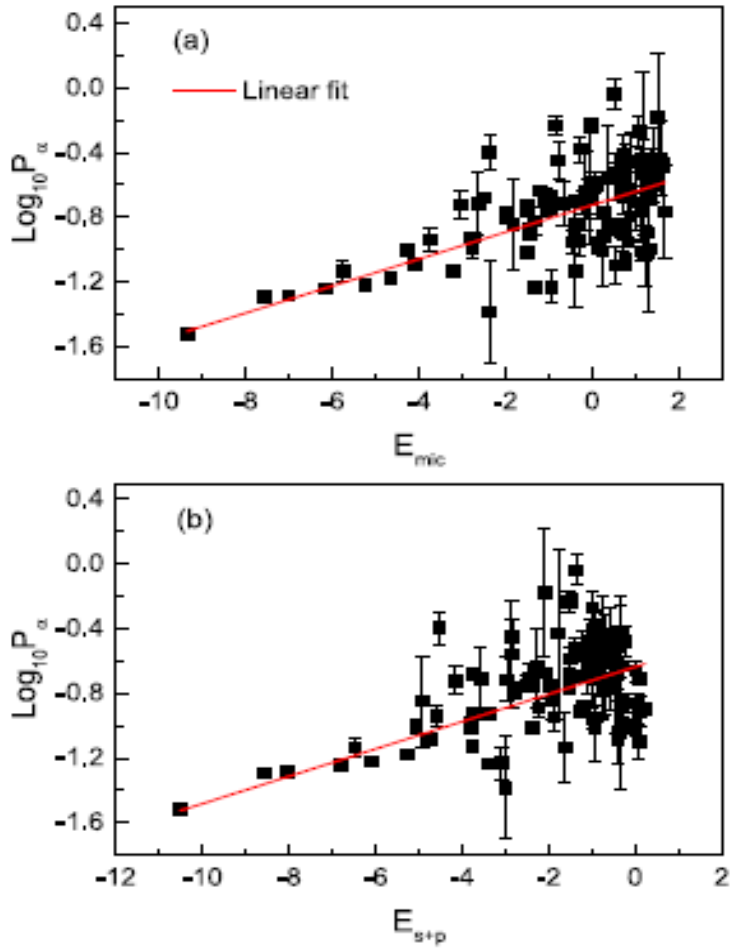
$$\Gamma = \frac{\hbar^2 k}{\mu}\left[\frac{\phi(\bar{r})}{G_\ell(k\bar{r})}\right]^2$$

$$T_{1/2} = \hbar \ln 2 / P_\alpha \Gamma$$

2. α decay of nuclei: nuclear structure

南京理工大学物理学院
SCHOOL OF PHYSICS , NANJING UNIVERSITY OF SCIENCE&TECHNOLOGY



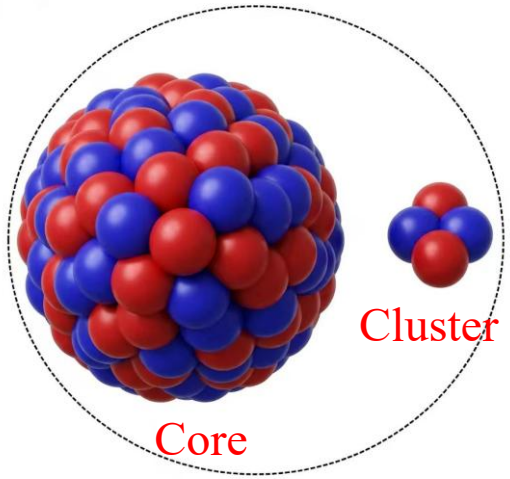


YB Qian and ZZ Ren, PLB 777, 298 (2018); JPG 45, 035103 (2018)

3. Cluster structure: two-body cluster model

南京理工大学 物理学院
SCHOOL OF PHYSICS , NANJING UNIVERSITY OF SCIENCE&TECHNOLOGY

Two-body cluster model



Schrödinger equation of the two-body system

$$\left(-\frac{\hbar^2}{2\mu}\nabla^2 + V(r)\right)|n,l,m\rangle = E_{nl}|n,l,m\rangle$$

$$\mathbf{V(r) = V_C(r) + V_N(r)}$$

Classic nuclear potentials: Woods–Saxon (level inversion), double-folding (level compression)

Nuclear potential used here: (1 + Gaussian)(W.S. + W.S.3)

$$V_N(r) = -V_0\left[1+\lambda\exp\left(-\frac{r^2}{\sigma^2}\right)\right]\left\{\frac{b}{1+\exp[(r-R)/a]} + \frac{1-b}{\{1+\exp[(r-R)/3a]\}^3}\right\}$$

Nucleus	Core + cluster configuration
^{20}Ne	^{16}O + α
^{44}Ti	^{40}Ca + α
^{52}Ti	^{48}Ca + α
^{60}Zn	^{56}Ni + α
^{94}Mo	^{90}Zr + α
^{136}Te	^{132}Sn + α
^{212}Po	^{208}Pb + α

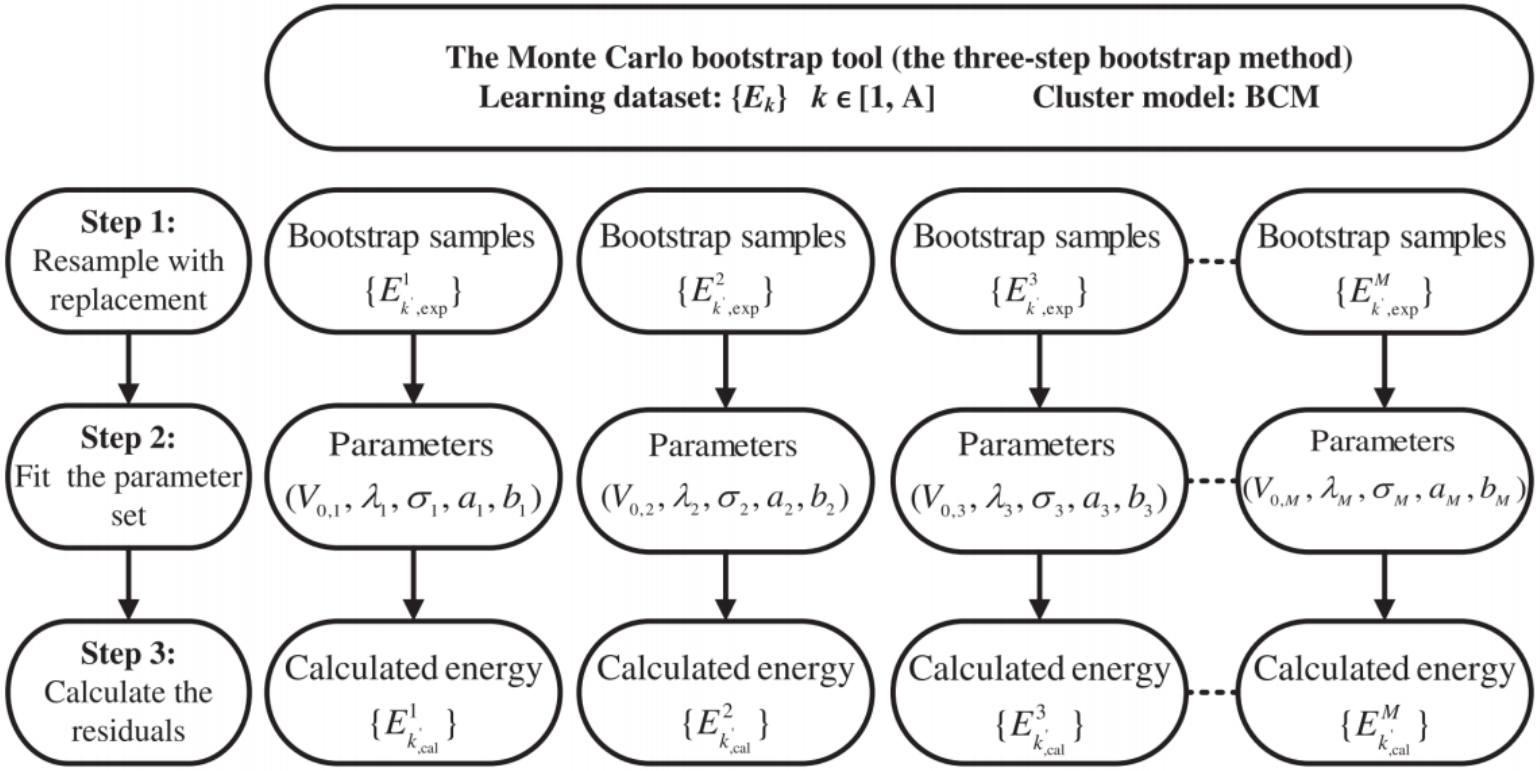
Existing literature: Doubly/semi-magic nuclei

1. Nuclear-potential parameters vary with the nucleus (universal?)

2. The calculation lacks error analysis (stable?)

3. Cluster structure: two-body cluster model

Bootstrap sampling strategy



Three-step bootstrap sampling flowchart

1. Take the A experimental energy levels of all nuclei as the learning set $\{E_k\}$; each time, resample with replacement to form a bootstrap sample set, the i-th sample being denoted $\{E^i_{k',\exp}\}$;

2. The bootstrap sample sets are used to fit the parameters of the nuclear potential

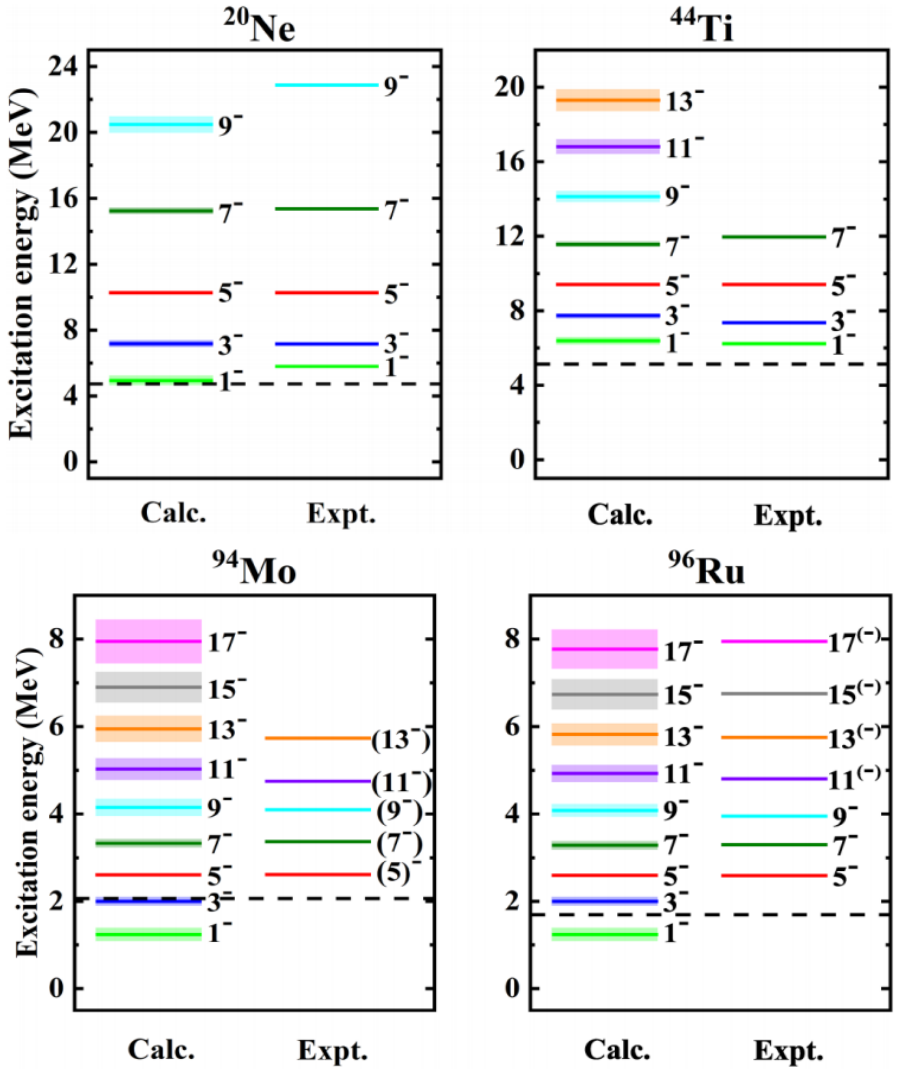
$$\chi^2_i = \frac{\sum_{i=1}^{A} \left(E^i_{k',\mathrm{cal}} - E^i_{k',\exp}\right)^2}{A}$$

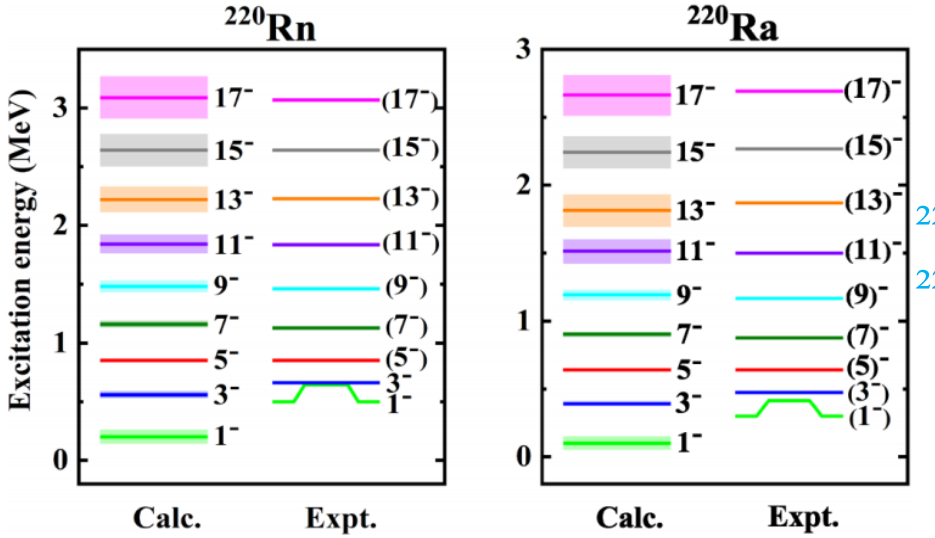
yielding one optimal parameter set;

3. Insert the optimal solution into the level calculation to obtain a set of level results. Repeating the procedure sufficiently many times gives the level distribution.

3. Cluster structure: two-body cluster model

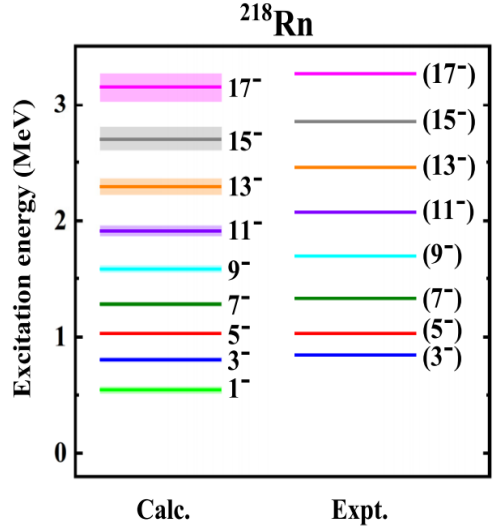
南京理工大学 物理学院
SCHOOL OF PHYSICS , NANJING UNIVERSITY OF SCIENCE&TECHNOLOGY





^{220}Rn: ^{12}Be + ^{208}Pb

^{220}Ra: ^{12}C + ^{208}Pb



^{218}Rn: ^{10}Be + ^{208}Pb

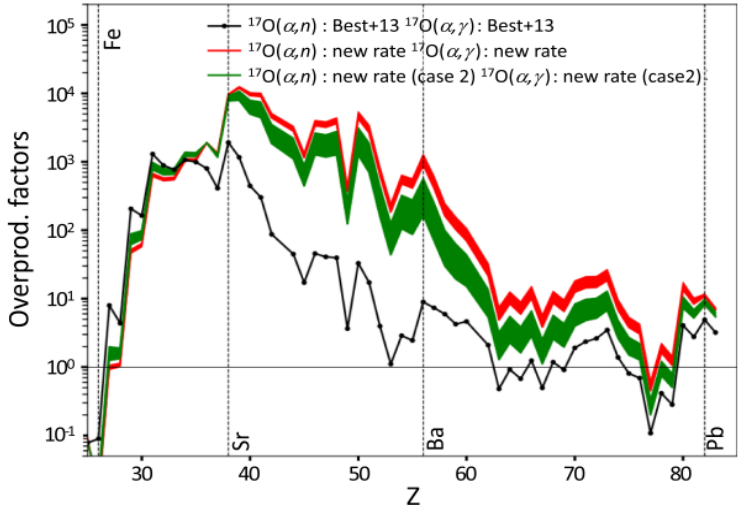
Negative-parity levels in heavy nuclei hint at cluster structure

Tao Wan, Yinbin Qian, PRC **110**, 014318 (2024)

3. Cluster structure: two-body cluster model

南京理工大学 物理学院
SCHOOL OF PHYSICS , NANJING UNIVERSITY OF SCIENCE&TECHNOLOGY

Cluster structure of odd-A nuclei from spin–orbit coupling



F. Hammache, et al., PRL **132**, 182701 (2024)

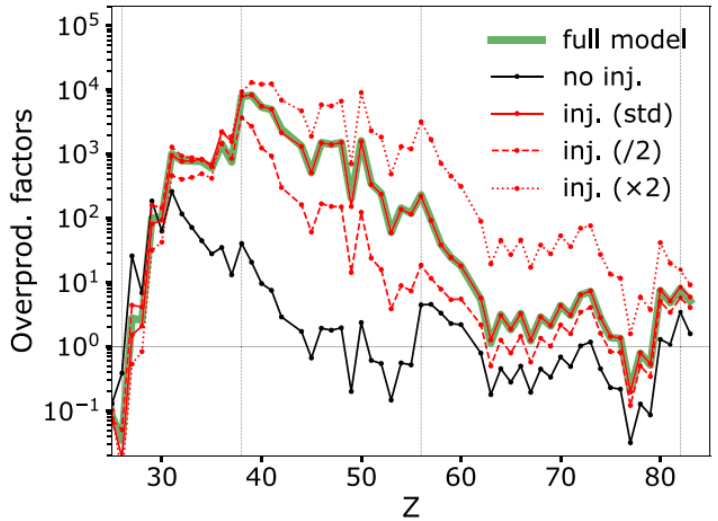
The level structure of ^{21}Ne near the α-particle threshold governs the cross section and effective flux of the stellar s-process ^{17}O(α, n) reaction

$$\left(-\frac{\hbar^2}{2\mu}\nabla^2 + V(r)\right)\left|n,l,m\right\rangle = E_{nl}\left|n,l,m\right\rangle$$

$$V(r) = V_N(r) + V_C(r) + V_{so}(r) + \frac{\hbar^2 l(l+1)}{2\mu r^2}.$$

Vso(r): spin–orbit coupling potential

$$V_{so}(r) = -V_{so}\left(\frac{\hbar}{m_\pi c}\right)^2 \frac{1}{r}\left|\frac{dV_N(r)}{dr}\right| l\cdot\sigma.$$



J. Frost-Schenk, et al., Mon. Not. R. Astron. Soc. **514**, 2650 (2022)

The resonant states of ^{19}F near the α threshold govern the cross section of the stellar ^{15}N(α, γ) radiative-capture reaction — the key to unravelling the origin of cosmic fluorine abundance.

Target nuclei:

^{19}F, ^{21}Ne, ^{43}Sc, ^{59}Cu, ^{93}Mo

Three-nucleon cluster "^{3}H or ^{3}He (σ)

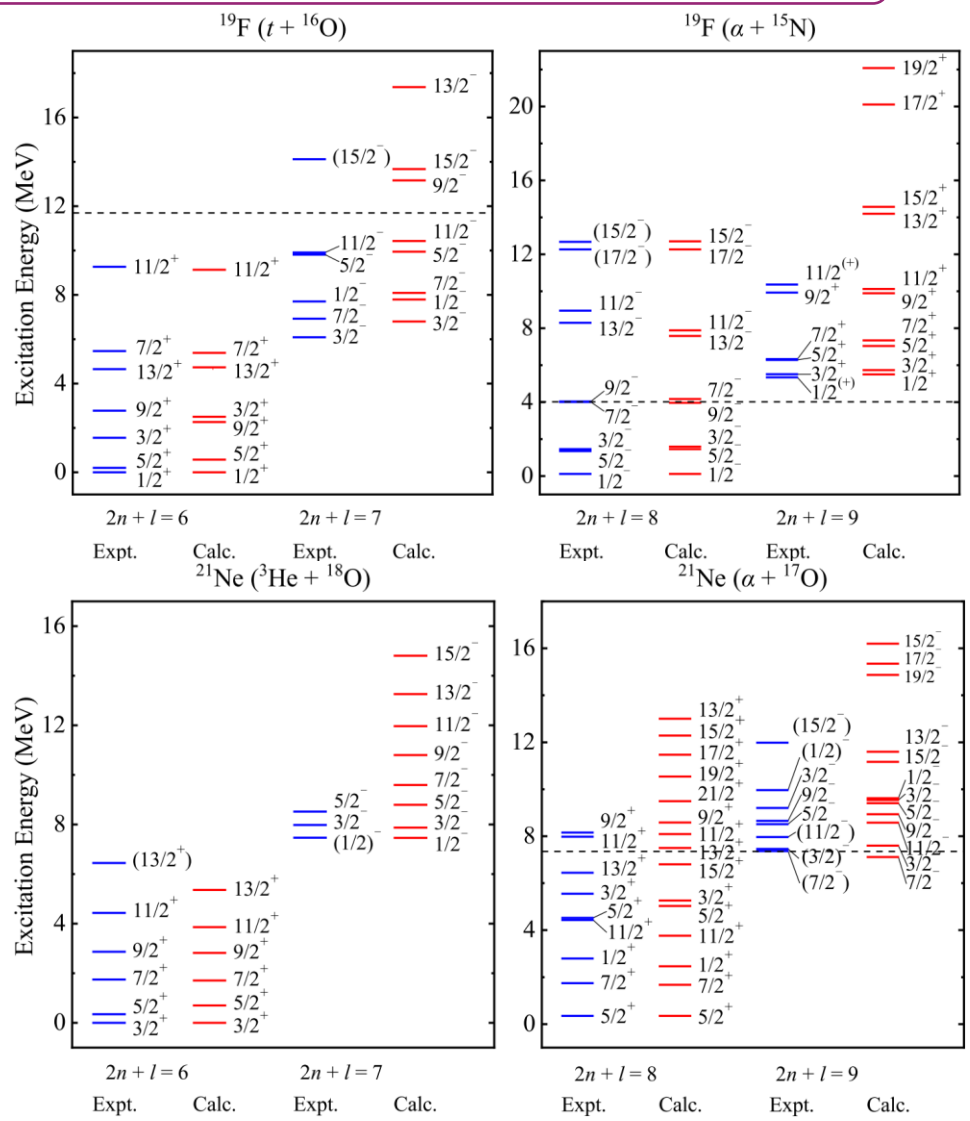
+ core"

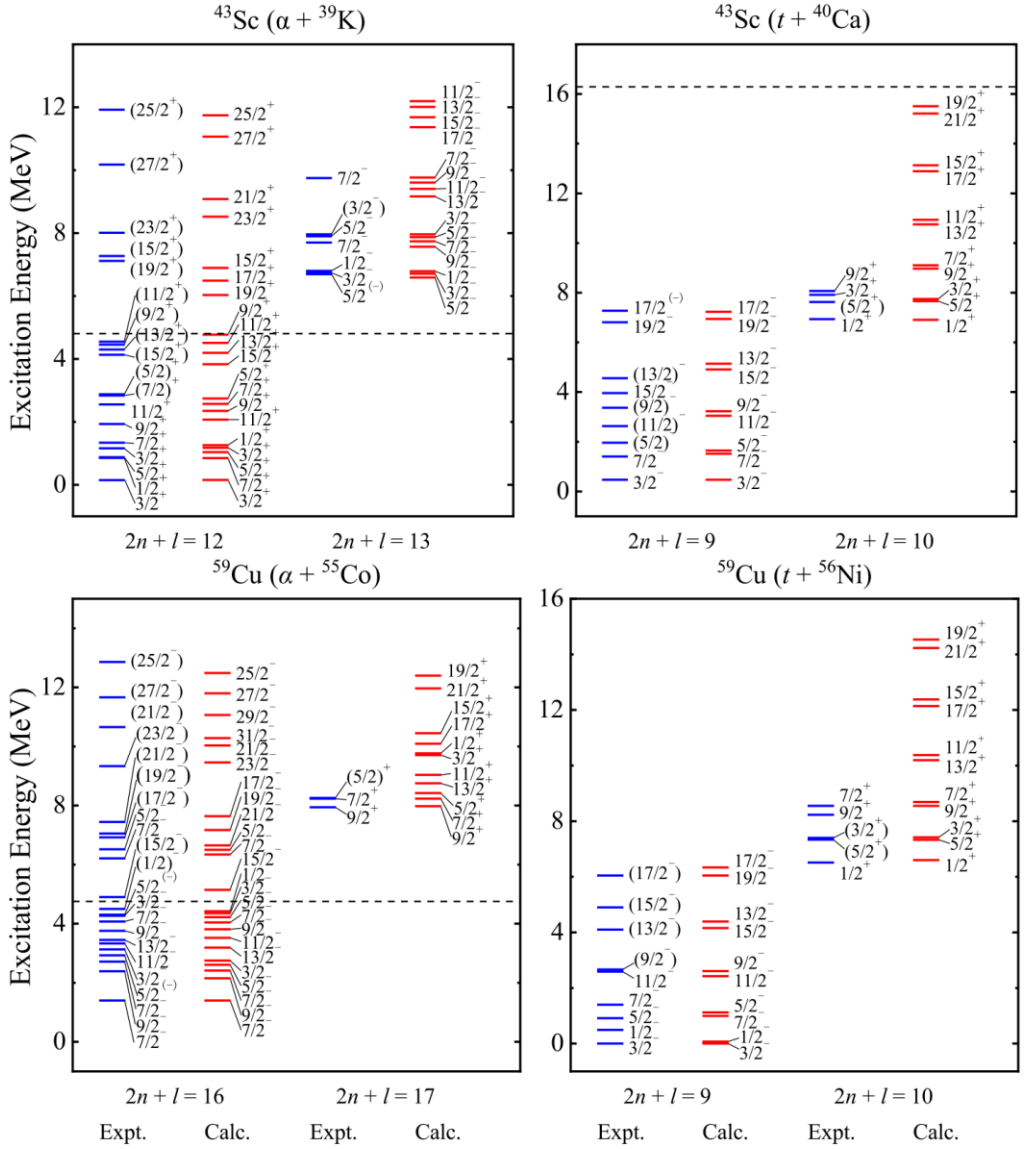
α cluster "α + core (σ)"

3. Cluster structure: two-body cluster model

南京理工大学 物理学院
SCHOOL OF PHYSICS , NANJING UNIVERSITY OF SCIENCE&TECHNOLOGY

Cluster structure of odd-A nuclei from spin–orbit coupling





Tao Wan, Yibin Qian, Chin. Phys. C **49**, 124103 (2025)

3. Cluster structure: two-body cluster model

南京理工大学 物理学院
SCHOOL OF PHYSICS , NANJING UNIVERSITY OF SCIENCE&TECHNOLOGY

Cluster structure of odd-A nuclei from spin–orbit coupling

B(E2) values of ^{19}F and ^{21}Ne

Nuclei (Cluster)	Transition	$B(E2)_{\text{calc.}}$	$B(E2)_{\text{expt.}}$	$B(E2)_1$
^{19}F(α)	$5/2^- \to 1/2^-$	19.53	21.60 ± 0.40	20.00
^{19}F(α)	$9/2^- \to 5/2^-$	26.36	28.00 ± 6.00	22.51
^{19}F(α)	$13/2^- \to 9/2^-$	23.56	19.00 ± 2.00	
^{19}F(α)	$11/2^- \to 7/2^-$	23.80	8.10 ± 2.00	23.88
^{19}F(t)	$5/2^+ \to 1/2^+$	5.36	6.95 ± 0.08	6.95
^{19}F(t)	$9/2^+ \to 5/2^+$	6.21	8.20 ± 0.90	8.09
^{19}F(t)	$13/2^+ \to 9/2^+$	3.93	3.20 ± 0.40	5.27
^{21}Ne(α)	$7/2^+ \to 5/2^+$	14.62	11.00 ± 4.00	
^{21}Ne(^{3}He)	$5/2^+ \to 3/2^+$	20.58	24.30 ± 2.00	24.16
^{21}Ne(^{3}He)	$7/2^+ \to 3/2^+$	7.04	9.30 ± 0.80	10.08
^{21}Ne(^{3}He)	$7/2^+ \to 5/2^+$	10.54	11.00 ± 4.00	15.10
^{21}Ne(^{3}He)	$9/2^+ \to 5/2^+$	10.90	15.70 ± 2.20	15.10
^{21}Ne(^{3}He)	$9/2^+ \to 7/2^+$	7.94	9.00 ± 5.00	9.87
^{21}Ne(^{3}He)	$11/2^+ \to 9/2^+$	2.85	6.00 ± 4.00	6.91

F. Ajzenberg-Selove, Nucl. Phys. A **392**, 1 (1983)
R. Firestone, Nucl. Data Sheets **127**, 1 (2015)
G. Lévai, Phys. Rev. C **44**, 166 (1991)

B(E2) values of ^{43}Sc and ^{59}Cu

Nuclei (Cluster)	$J_i^\pi(E_i^{\text{expt.}})$	$J_f^\pi(E_f^{\text{expt.}})$	$B(E2)_{\text{calc.}}$	$B(E2)_{\text{expt.}}$
^{43}Sc(α)	$5/2^+(0.881)$	$3/2^+(0.152)$	23.08	13.00 ± 5.00
^{43}Sc(α)	$3/2^+(1.159)$	$1/2^+(0.856)$	13.56	<180.00
^{43}Sc(α)	$3/2^+(1.159)$	$5/2^+(0.881)$	34.80	<180.00
^{43}Sc(α)	$7/2^+(1.338)$	$3/2^+(0.152)$	9.56	20.00 ± 9.00
^{43}Sc(α)	$7/2^+(1.338)$	$5/2^+(0.881)$	14.42	46.00 ± 24.00
^{43}Sc(α)	$9/2^+(1.933)$	$5/2^+(0.881)$	13.79	15.00 ± 4.00
^{43}Sc(α)	$9/2^+(1.933)$	$7/2^+(1.338)$	9.00	3.30 ± 1.60
^{43}Sc(α)	$11/2^+(2.554)$	$7/2^+(1.338)$	16.17	20.00 ± 3.00
^{43}Sc(t)	$7/2^-(1.408)$	$3/2^-(0.473)$	2.62	24.00 ± 9.00
^{43}Sc(t)	$5/2^-(1.963)$	$3/2^-(0.473)$	6.30	4.40 ± 2.50
^{43}Sc(t)	$11/2^-(2.635)$	$7/2^-(1.408)$	4.09	43.00 ± 16.00
^{59}Cu(t)	$1/2^-(0.492)$	$3/2^-(0)$	4.83	<300.00
^{59}Cu(t)	$5/2^-(0.914)$	$3/2^-(0)$	0.66	<2.90
^{59}Cu(t)	$7/2^-(1.399)$	$3/2^-(0)$	2.98	17.00 ± 8.00
^{59}Cu(t)	$7/2^-(1.399)$	$5/2^-(0.914)$	0.34	1.30 ± 0.80

B. Singh, Nucl. Data Sheets **126**, 1 (2015)
M. Shamsuzzoha Basunia, Nucl. Data Sheets **151**, 1 (2018)
C.M. Baglin, Nucl. Data Sheets **112**, 1163 (2011)
Tao Wan, Yibin Qian, Chin. Phys. C **49**, 124103 (2025)

三、重核集团结构：3. 集团态耦合

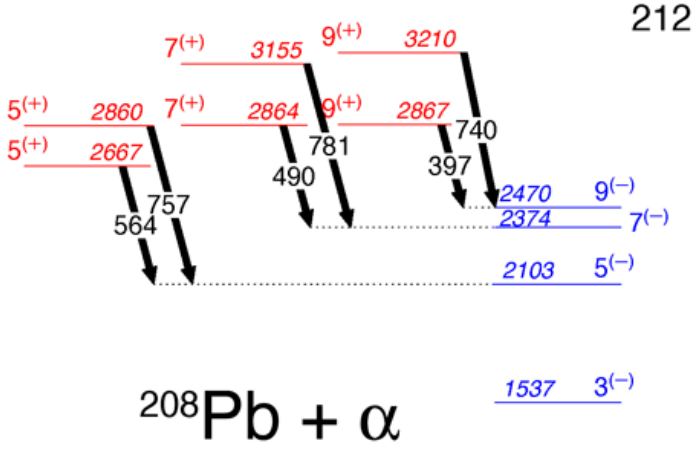
PRL 104, 042701 (2010) Selected for a Viewpoint in *Physics*
PHYSICAL REVIEW LETTERS
week ending 29 JANUARY 2010

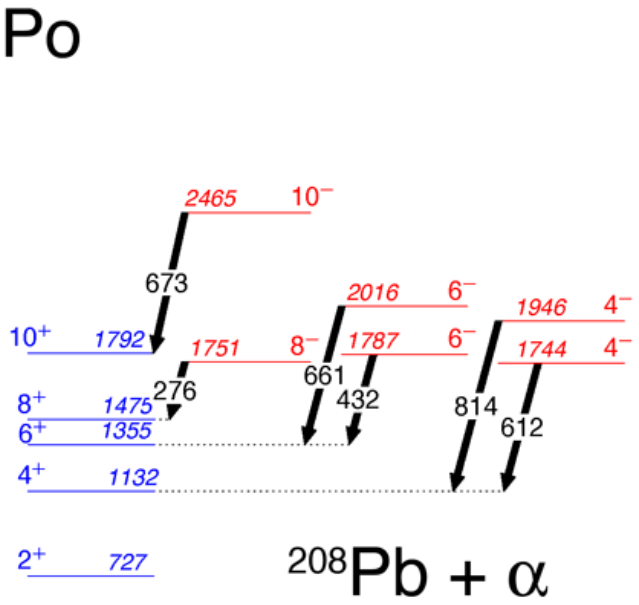
Novel Manifestation of α-Clustering Structures: New "α + ^{208}Pb" States in ^{212}Po Revealed by Their Enhanced $E1$ Decays

A. Astier,[1] P. Petkov,[1,2] M.-G. Porquet,[1] D. S. Delio
[1]*CSNSM, IN2P3-CNRS and Université Paris-Sud, 91*
[2]*Institute for Nuclear Research and Nuclear Energy, Bulgarian Acaden*
[3]*Horia Hulubei National Institute of Physics and Nuclear Engineering 407*
[4]*Academy of Romanian Scientists, 54 Splaiul Independentei, 0*
[5]*IPN, IN2P3-CNRS and Université Paris-Sud, 9140*
(Received 15 September 2009; published 25 Ja

Excited states in ^{212}Po were populated by α transfer using the ^{2} deexcitation γ rays were studied with the Euroball array. Several level $E1$ transition ($E_\gamma < 1$ MeV) populating the yrast state with the sam measured by the Doppler-shift attenuation method. The values, found i enhanced transitions, $B(E1) = 2 \times 10^{-2}$–1×10^{-3} W.u. These resu α-cluster structure which gives rise to states with non-natural-parity v system cannot rotate collectively, as expected in the "α + ^{208}Pb" case motion of the α-core distance are observed for the first time.

DOI: 10.1103/PhysRevLett.104.042701 PACS numbers: 2







shell model

三、重核集团结构：3. 集团态耦合

PHYSICAL REVIEW C **104**, 054316 (2021)

Reinterpretation of excited states in ^{212}Po: Shell-model multiplets rather than α-cluster states

A. Fernández,[1] A. Jungclaus,[1,*] P. Golubev,[2] D. Rudolph,[2] L.
A. Gadea,[6] E. Nácher,[1] A. Perea,[1] K. Wimmer,[1] E. Clément,[7]
A. Lemasson,[7] H. J. Li,[7] J. Ljungvall,[5] L. Ménager,[7] R. M. Pé
A. Såmark-Roth,[2] G. S. Simpson,[8] C. Spitaels,[7] M. Zielinska,
N. Lalović,[2] Ch. Lorenz,[2] B. Quintana,[13] G. Rainovski,
B. Birkenbach,[16] A. J. Boston,[17] H. C. Boston,[17] A.
C. Domingo-Pardo,[6] J. Eberth,[16] V. González,[20] L. J. Harkness
A. Maj,[19] R. Menegazzo,[22] D. Mengoni,[22,23] C. Michelagno

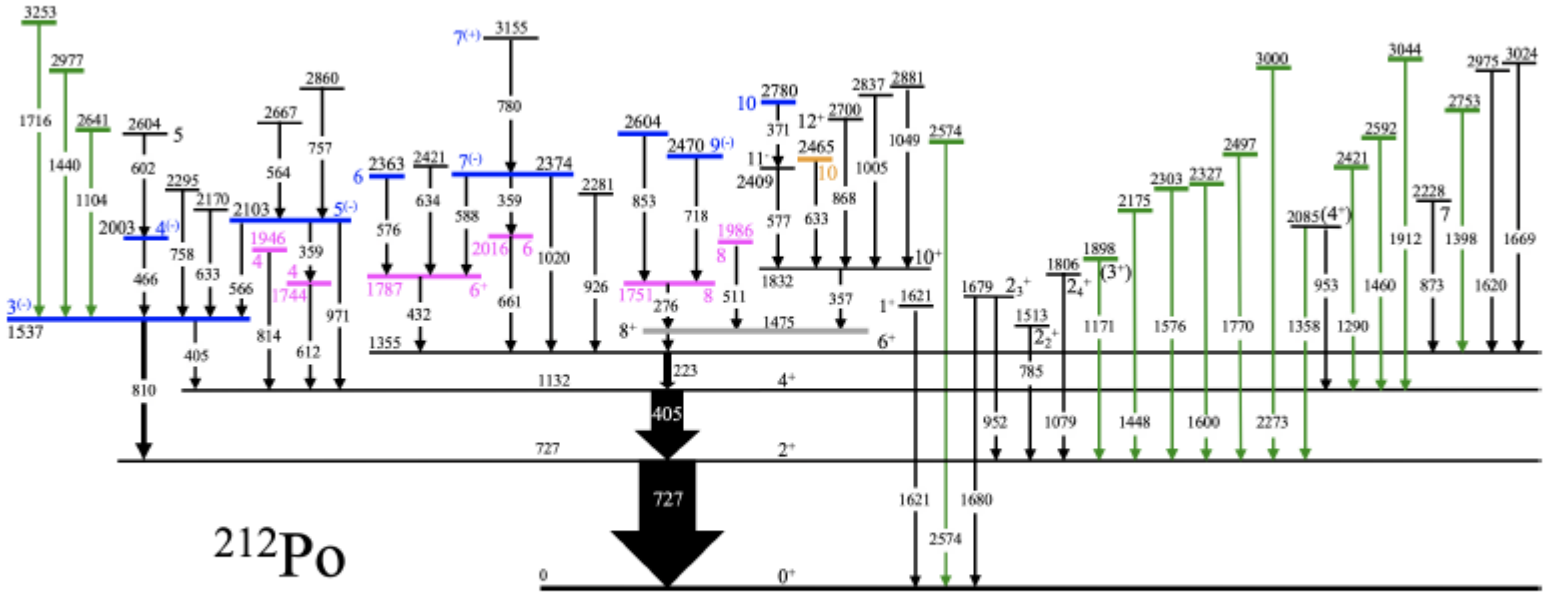


FIG. 10. Partial excitation scheme of ^{212}Po. Newly identified γ rays and excited states are shown in green. Following the color code introduced in Ref. [5], the negative-parity states discussed in the text are highlighted in pink, blue, and orange. Note that in the present work, the negative parity of the UPD shown in pink is questioned. The isomeric 8^+ state at 1476 keV ($T_{1/2} = 14.6(3)$ ns [25]) is shown as thick gray line. When available, the transition and level energies as well as spin assignments were adopted from Ref. [5].

三、重核集团结构：3. 集团态耦合

$$\Psi_{JM} = \sum_{IL} C^J_{IL} \psi_{ILJM},$$

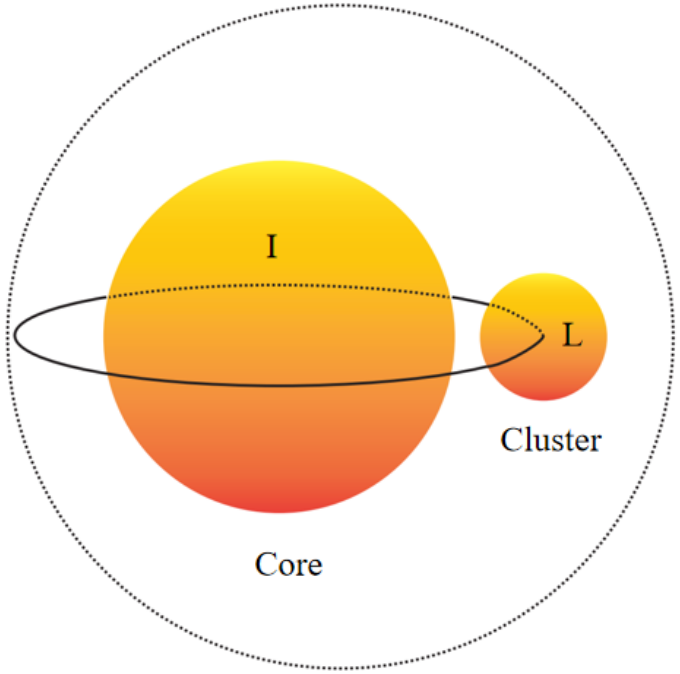
$$\psi_{ILJM} = \phi(\alpha)[\phi_I(\mathrm{Pb}) Y_L(\hat{r})]_{JM} \chi^J_{IL}(r),$$

$$\begin{aligned}\langle \psi_{I'L'JM}|H|\psi_{ILJM}\rangle &= E^J_{IL}\delta_{I,I'}\delta_{L,L'} + \sum_{\ell=2,3}(-1)^{\ell+I+L}\sqrt{(2I+1)(2L'+1)} \\ &\times \langle I0I'0|\ell 0\rangle \langle L0L'0|\ell 0\rangle U(I\ell JL'; I'L)\beta^J_{\ell II'},\end{aligned}$$

with

$$E^J_{IL} = \langle \chi^J_{IL}|T_L + V_0|\chi^J_{IL}\rangle + \epsilon_I,$$

$$\beta^J_{\ell II'} = (\kappa_{I'}/4\pi)\langle \chi^J_{I'L'}|V_\ell|\chi^J_{IL}\rangle,$$



Theoretical treatment on α decay of ^{146}Sm

α-core interaction potential of the cluster model:

$$V_N(r) = -V_0[1+\lambda\exp(-\frac{r^2}{\sigma^2})]\times\{\frac{x}{1+\exp[(r-R)/a]}+\frac{1-x}{1+\exp[(r-R)/3a]^3}\} \quad (1)$$

A new technique for calculating decay width:

$$u_{n\ell m}(r) \backsimeq A(G_\ell(kr)+iF_\ell(kr)) \longrightarrow Aexp(ikx+\delta) \quad (2)$$

$$\Gamma = \frac{\hbar^2 k}{\mu}A^2 \quad (3)$$

$$A^2 = \lim_{r\to\infty}|\Psi_{n\ell m}(r)|^2 = \frac{2A_1^2A_2^2}{A_1^2+A_2^2} \quad (4)$$

As for the half-life:

$$T_{1/2} = \hbar\ln 2/P_\alpha\Gamma \quad (5)$$

二、原子核的α衰变：对关联简介

南京理工大学 物理学院
SCHOOL OF PHYSICS，NANJING UNIVERSITY OF SCIENCE&TECHNOLOGY

支持 T=0 静态配对的证据

① Wigner 能量 (N=Z 核额外结合能)

N=Z 奇奇核 ~2–3 MeV 额外结合能

→ 归因于 T=0 np 对关联

② N=Z 奇奇核低激发谱

^{42}Sc: T=1 基态(0^+) vs T=0 1^+ ~0.6 MeV

T=1/T=0 能级近简并 → 两种配对共存

③ 对转移反应增强

N=Z 核中 np 对转移截面异常增大

→ T=0 配对的动力学信号

④ SO(8) 对称性模型

T=0+T=1 配对在 SO(8) 极限下等价于

α-like 四重子凝聚 → 配对-集团对偶

⑤ 壳模型 Monte Carlo (SMMC)

pf 壳 N=Z 核 → T=0 对关联信号显著

质疑 T=0 静态凝聚的证据

① T=1 基态普遍占优

绝大多数 N=Z 奇奇核基态为 T=1 (0^+)

→ $^1S_0$ 吸引主导，T=0 配对未凝聚

② 缺少清晰"对能隙"信号

无类似 T=1 的 OES 信号 → 无静态凝聚

对转移截面增强也可用动力学解释

③ $^3S_1$ 吸引弱于 $^1S_0$

氘核仅 2.2 MeV 束缚 → 配对凝聚弱

$^3P_1$ 道排斥 → 自旋-轨道耦合抑制 T=0

④ DFT/EDF 计算结果

多数 HFB 计算 → T=0 静态对凝聚不稳定

仅当人工增强 T=0 对力时才出现

⑤ 中子过剩时 Pauli 阻塞

离开 N=Z 线 → T=0 配对迅速消失

→ 非普遍现象，仅为局域关联

五、np 配对争论：理论现状与关键文献

Current theoretical status & key references

当前主流共识 (2020s)

- T=1 np 配对 (J=0): 存在性无争议，作为 T=1 同位旋三重态 Tz=0 成员 → 已在 N≈Z 核中确认
- T=0 np 配对 (J=1): 存在强动力学关联，但静态 Cooper 对凝聚的证据不充分
- **主流观点: T=0 配对是重要的"动力学关联"而非"静态凝聚"——对 N=Z 核性质有显著影响但不形成超流**
- 少数观点: 在特定核区 (pf 壳 N=Z) 可能存在 T=0 静态凝聚 → 需更多实验证据

关键文献

- Goodman, Adv. Nucl. Phys. 11, 263 (1979)
  → T=0/T=1 配对竞争的经典综述
- Dean & Hjorth-Jensen, RMP 75, 607 (2003)
  → 壳模型中的配对: T=0 vs T=1
- Frauendorf & Macchiavelli, PPNP 78, 24 (2014)
  → T=0 配对综述: 证据与开放问题
- Sagawa, Tanimura, Hagino, PRC 87, 034310 (2013)
  → N=Z 核中 T=0 配对的对转移探针

开放问题

① T=0 对凝聚的明确实验信号是什么?
② 如何在 HFB/DFT 中自洽包含 T=0 配对?
③ 远离 N=Z 线是否有 T=0 配对残留?
④ T=0 配对在 α 集团形成中起什么作用?
⑤ 下一代放射性束装置 (HIAF, FRIB) 能否提供决定性实验证据?

Pauli 原理对配对通道的完整约束

L+S+T = 奇数 → 哪些 (L,S,T) 组合是允许的?

两核子配对通道的 Pauli 允许性分析

配对道	L	S	T	L+S+T	允许?	J	核子类型	备注
$^1S_0$ (T=1)	0	0	1	1(奇)	✓	0	pp,nn,np	最强吸引, 主导配对
$^3S_1$+$^3D_1$ (T=0)	0+2	1	0	1(奇)	✓	1	仅 np	氘核型, 弱于$^1S_0$
$^3P_0$ (T=0)	1	1	0	2(偶)	✗	—	—	Pauli 禁止!
$^3P_1$ (T=1)	1	1	1	3(奇)	✓	1	pp,nn,np	$^3P_1$ 排斥 → 不形成对
$^1P_1$ (T=0)	1	0	0	1(奇)	✓	1	仅 np	弱吸引, 不主导
$^1D_2$ (T=1)	2	0	1	3(奇)	✓	2	pp,nn,np	高角动量, 次要
$^3D_2$ (T=0)	2	1	0	3(奇)	✓	2	仅 np	张量力耦合

关键结论:

① T=1 配对: $^1S_0$ (J=0) 是最低允许道 → 最强吸引 → 遍布全核素图

② T=0 配对: $^3S_1$+$^3D_1$ (J=1) 是最低允许道 → 吸引较弱 → 仅 N≈Z 区

③ 配对道的角动量 J 由 Pauli 原理 + NN 相互作用共同决定 → 不总是 J=0!

④ $^3P_1$ (T=1) 虽 Pauli 允许但核力排斥 → 核力选择与 Pauli 约束同等重要

五、np 配对是否存在的争论：问题综述

★ T=0 静态对凝聚 — 核结构中的一个核心开放问题

争论的核心

T=1 np 配对 ($^1S_0$, J=0) 作为同位旋三重态 Tz=0 成员 → 存在性无争议

但 T=0 np 配对 ($^3S_1$+$^3D_1$, J=1) 是否形成静态 Cooper 对凝聚?

为什么这是一个困难的问题?

1. T=0 道的 $^3S_1$ 吸引弱于 $^1S_0$ → 对能隙可能太小而无法形成凝聚
2. T=0 配对仅当质子和中子费米面接近时 (N≈Z) 才可能 → 可用核素范围窄
3. 实验信号不明确: 无类似 T=1 配对的清晰"对能隙"信号
4. 理论方法依赖: 不同多体方法给出不同结论 (壳模型 vs DFT vs SMMC)
5. 自旋-轨道耦合 ($^3P_1$ 排斥) → 可能抑制 T=0 配对的集体性

争论的核心可归结为: T=0 配对的关联是"静态凝聚"还是"动力学关联"?

六、α 集团形成动力学中的对关联角色

Pairing as the microscopic driver of α-cluster formation

配对→集团: 微观机制

1. BCS 对关联 → 时间反演轨道上的核子对
2. 表面配对增强 → 低密度表面区对关联最强
   (核内部密度高, Pauli 阻塞抑制配对)
3. 四核子关联 (Quarteting) → 2p+2n 共振
4. α-like 组态在表面自组织 → 类 α 集团
5. 量子隧穿 → α 衰变 (Gamow 理论)

关键: 对关联提供形成集团的"种子"

无对关联 → 独立粒子运动 → 无 α 集团

配对-集团对偶性 (SO(8) 图像)

SO(8) 代数: 包含 T=0+T=1 配对算符

配对极限 ↔ 四重子凝聚极限

G (对力强度) vs Kq (四重子力强度)

G 主导 → BCS 对凝聚 (超流相)

Kq 主导 → α-like 四重子凝聚

中间 → 配对与集团共存竞争

→ T=0 np 配对可能是连接两种极限的

关键桥梁!

微观集团模型中的对关联处理

方法	对关联处理	α 集团描述
GCM (生成坐标)	投影 BCS 态 → 对关联包含在基态	生成坐标 = 集团间距
RGM (共振群)	壳模型组态混合 → 隐含配对关联	Pauli 允许的集团-核相对运动
THSR (容器模型)	对关联在容器态中自然出现	α 粒子在共同容器中 Bose 凝聚
AMD+BCS	反对称分子动力学 + BCS 对关联	波包描述 + 集团形成动力学

结论: 现代微观集团模型必须在统一框架中同时处理对关联和集团自由度

六、Hoyle 态与 α 凝聚：配对-集团对偶性的范例

^{12}C Hoyle state — the paradigm of α condensation & pairing-cluster duality

^{12}C 的 Hoyle 态 (7.654 MeV, 0^+_2)

- 1954: Hoyle 预言其存在 → 解释恒星中 $^3\alpha \rightarrow ^{12}$C 的 triple-α 过程
- 结构: 3个 α 粒子在共同 0s 轨道上 → Bose-Einstein 凝聚 (BEC)
- THSR 波函数 (2001): $|\Psi\rangle \propto \int dR\, \exp(-R^2/\beta^2)\, [\Phi\alpha_1(R)\Phi\alpha_2(R)\Phi\alpha_3(R)]$

配对视角的 Hoyle 态

- 每个 α 粒子 = 2 个 T=1 Cooper 对
- Hoyle 态 = 6 个配对核子的相干态
- **对关联 → 四核子关联 → α 凝聚**
- 配对能隙 ≈ α 凝聚序参量
- 激发 Hoyle 态 ↔ 打开对能隙

推广: Nα 凝聚态

- ^{16}O: 4α 凝聚的 Hoyle-like 态?
- ^{20}Ne, ^{24}Mg: α 凝聚链?
- **Nα 凝聚 → 低密度核物质的新相**
- 对关联超流 ↔ α 凝聚相变
- 中子星内壳层: 对凝聚→α 凝聚?

核心启示

对关联和 α 集团形成是同一物理现象的两个侧面: 配对是"微观"描述 (核子语言), α 凝聚是"宏观"描述 (集团语言)。
两者的统一是核多体理论的重大进展, 也是理解天体核过程 (triple-α, α 过程) 的关键。

六、研究前沿：对关联与 α 集团

Pairing–α cluster connection: current frontiers

前沿方向 ①: T=0 配对探针

- N=Z 核 np 对转移反应
- 奇奇核 T=1/T=0 能级系统学
- β 衰变中的对关联信号
- γ 跃迁中的配对矩阵元
- **新装置: HIAF, FRIB, FAIR**

前沿方向 ②: α 预形成的微观

- 从头算 (ab initio): CC, IMSRG
  → 无参数预形成振幅计算
- 壳模型 Monte Carlo (SMMC)
  → 有限温度 α 预形成
- 核子-核子对关联的对转移
  → 四核子对转移 (^{6}Li, d) 等

前沿方向 ③: 天体核过程

- Triple-α 反应率 + 配对效应
- α 过程 (αp, αn 反应)
- 中子星内壳层: 超流→凝聚
- 核 pasta 相中的对关联
- X 射线暴中的 α 分离能

2. α decay of nuclei: pairing correlations

南京理工大学 物理学院
SCHOOL OF PHYSICS , NANJING UNIVERSITY OF SCIENCE&TECHNOLOGY

α-preformation amplitude

$$F\alpha(R) = \langle \Phi(A-4) \times \varphi\alpha \mid \Psi(A) \rangle$$

- Φ(A−4): daughter-nucleus wave function
- φα: intrinsic α-particle wave function $(0s)^4$
- Ψ(A): parent-nucleus wave function

How does pairing enhance Fα?

① BCS pairing → nucleon pairs spread around the Fermi surface
→ enhanced four-nucleon correlations in the surface region
② Surface projection of pair condensation → larger γ^2/γ^2_W
(reduced width / Wigner limit)
③ Mang (1960): shell model + pairing
→ α formation amplitude enhanced by a factor of 2–5
④ Delion et al. (1992): BCS approach
Systematically large γ^2 for N > 126 → evidence for pair condensation

Key relations

α-decay width:

$$\Gamma\alpha = \gamma^2(R) \times P(R)$$

- $\gamma^2(R)$: reduced width (preformation probability)
- P(R): penetration factor (Gamow)

Effect of pairing:

$P\alpha \propto |F\alpha(R)|^2 \propto$ pairing strength

Temperature dependence:

- Tc ≈ 0.57 Δ (BCS critical temperature)
- T > Tc: the pairing gap vanishes
  → α preformation probability changes
  → temperature dependence of α decay from excited states

Isospin window:

- T=1 pp + T=1 nn → T=0 (α)
- **Can T = 0 np pairs accelerate preformation?**
  → open question!